Journal of Volcanology and Geothermal Research 273 (2014) 41–57

Contents lists available at ScienceDirect

Journal of Volcanology and Geothermal Research

journal homepage: www.elsevier.com/locate/jvolgeores

The chemistry and element fluxes of the July 2011 Múlakvísl and Kaldakvísl glacial floods, Iceland

Iwona Galeczka [a,1], Eric H. Oelkers [a,b], Sigurdur R. Gislason [a]

[a] Institute of Earth Sciences, University of Iceland, Sturlugata 7, 101 Reykjavik, Iceland
[b] GET–UMR 5563 CNRS Université Paul-Sabatier IRD, 14, Avenue Edouard Belin, 31400 Toulouse, France

ARTICLE INFO

Article history:
Received 26 August 2013
Accepted 19 December 2013
Available online 3 January 2014

Keywords:
Subglacial floods
Reaction path modelling
Dissolved and particulate element transport

ABSTRACT

This study describes the chemical composition and fluxes of two ~2000 m^3/s glacial floods which emerged from the Icelandic Mýrdalsjökull and Vatnajökull glaciers into the Múlakvísl and Kaldakvísl rivers in July 2011. Water samples collected during both floods had neutral to alkaline pH and conductivity from 100 to 900 μS/cm. The total dissolved inorganic carbon (DIC), present mostly as HCO_3^-, was ~9 mmol/kg during the flood peak in the Múlakvísl but stabilized at around 1 mmol/kg; a similar behaviour was observed in the Kaldakvísl. Up to 1.5 μmol/kg of H_2S was detected. Concentrations of most of the dissolved constituents in the flood waters were comparable to those commonly observed in these rivers. In contrast, the particulate suspended material concentration increased dramatically during the floods and dominated chemical transport during these events. Waters were supersaturated with respect to a number of clays, zeolites, carbonates, and Fe hydroxides. The most soluble elements were Na, Ca, K, Sr, Mn, and Mg, whereas the least soluble were Ti, Al, and REE. This is consistent with the compositions of typical surface waters in basaltic terrains and the compositions of global rivers in general. The toxic metal concentrations were below drinking water limits, suggesting that there was no detrimental effect of flood waters chemistry on the environment. Increased concentration of DOC, formate, and acetate in the flood waters suggests substantial subglacial microbiological activity in the melt water prior to the floods. Reaction path modelling of the flood water chemical evolution suggests that it experienced subglacial water–rock interaction for at least a year in the presence of limited amounts of acid gases (e.g. SO_2, HCl and HF). This suggests that the heat source for glacier melting was geothermal rather than volcanic.

1. Introduction

Iceland is the largest landmass found above sea level at mid-ocean ridges. There are over 30 active volcanic systems with a total average eruptive frequency of at least 20 eruptions per century and magma output rate of 5 km^3 per century (Thordarson and Höskuldsson, 2008). High-temperature geothermal systems are located in the central parts of active volcanic and rifting belts with only three located close to their margins (Arnórsson et al., 2008). Due to elevation and favourable location with respect to humid air masses, the most active volcanoes and geothermal areas in Iceland are covered by glaciers. The heat from subglacial magma intrusions and exothermic rock alteration reactions melts the overlying ice, forming depressions in the glaciers called cauldrons (Steinthórsson and Óskarsson, 1986; Björnsson, 2003). Melt water often collects at the base of the glacier; eventually there may be sufficient melt water to lift the ice, resulting in a glacial flood. There are two main causes of glacial floods — called jökulhlaups in Icelandic[2]: (1) subglacial geothermal activity during which ice is melted continuously and accumulates in periodically drained subglacial lakes and, (2) subglacial volcanic eruptions where melt water is produced rapidly due to thermal energy released during magma cooling and fragmentation (Gudmundsson et al., 2008). The former tend to be smaller in volume and more common than the floods originating from volcanic eruptions (Björnsson and Kristannsdottir, 1984; Gudmundsson et al., 2005, 2008). Drainage occurs during semi-regular intervals and not all flood events are detected. During subglacial volcanic eruptions, floods can be abrupt, loaded with suspended particulate material, and sometimes can contain high concentrations of dissolved metals and volatiles (Kristmannsdóttir et al., 1999; Gislason et al., 2002; Snorrason et al., 2002; Stefánsdóttir and Gíslason, 2005; Sigfússon, 2009). Some of these floods can be of 'Amazonian' size; with maximum flow rates of 3000–700,000 m^3/s (e.g. the glacial flood from Katla in 1918 and the glacial flood in the Jökulsa a Fjöllum between 2500 and 2000 years ago; Tómasson, 1996; Snorrason et al., 2002; Waitt, 2002; Gudmundsson et al., 2005; Russell et al., 2010). Because of their

E-mail address: img3@hi.is (I. Galeczka).
[1] Tel.: +354 525 5414; fax: +354 562 9767.

[2] In Icelandic 'jökull' is a glacier, and 'hlaup' means flood.

0377-0273/$ – see front matter © 2013 Elsevier B.V. All rights reserved.
http://dx.doi.org/10.1016/j.jvolgeores.2013.12.004

potentially large impact on the environment, glacial floods have been extensively studied with respect to natural hazards, fluid mechanics, sediments, dissolved constituents, and suspended particulate transport (Gudmundsson et al., 1997; Maizels, 1997; Björnsson, 1998, Kristmannsdóttir et al., 1999; Geirsdóttir et al., 2000; Roberts et al., 2000; Gislason et al., 2002; Björnsson, 2003; Alho et al., 2005; Stefánsdóttir and Gíslason, 2005; Russell et al., 2006, 2010).

The chemical composition of waters affected by geothermal and volcanic activity (groundwaters, surface waters and flood waters) is influenced by its interaction with surrounding rocks, heat, and gas supply, and overburden pressure which affects gas solubility. During subaerial volcanic eruptions, the proton and metal salts adsorbed on tephra surface will dissolve when exposed to rain- and surface-waters (Frogner et al, 2001; Delmelle et al., 2007; Flaathen and Gislason, 2007; Jones and Gislason, 2008; Gislason et al., 2011; Olsson et al., 2013). The metal salts are commonly sulphates, fluorides, and chlorides, which originate from magmatic gases such as SO_2, HF, and HCl (Óskarsson, 1980, 1981; Seymonds and Reed, 1993). The dissolution of salts releases these metals and protons. This might significantly increase the concentrations of some elements, including F and Al, leading the fluids to be toxic (Flaathen and Gislason, 2007). During subglacial eruptions, some portion of the magmatic gases dissolves directly into the melt waters affecting the flood water chemical composition (Gislason et al., 2002; Sigfússon, 2009). Numerous studies have focused on the role of volcanic and geothermal degassing on the mobilization of rock constituents in surface- and groundwaters (Federico et al., 2002, Aiuppa et al., 2003; Cioni et al., 2003, Marini et al., 2003; Federico et al., 2004; Aiuppa et al., 2005; Taran et al., 2008; Flaathen et al., 2009; Ambrosio et al., 2010; Floor et al., 2011). Some of these studies confirm that the input of magmatic gases, including CO_2, may promote host rock dissolution increasing significantly dissolved metal concentrations (e.g. Federico et al., 2002, 2004; Flaathen et al., 2009; Oskarsdottir et al., 2011). Increased host rock dissolution may, however, have a positive impact on the biota due to the addition of limiting elements to the fluid, potentially leading to short lived net flux of CO_2 from the atmosphere (Gislason et al., 2002). If water–rock interaction is sufficient, the water can be neutralised leading to the precipitation of metal scavenging (oxy)hydroxides and other secondary phases (Aiuppa et al., 2000a,b, 2005; Flaathen and Gislason, 2007; Flaathen et al., 2009; Kaasalainen and Stefánsson, 2012).

An improved understanding of glacial floods is of wide interest for several reasons. Firstly, the heat source origin is critical to the potential environmental impact of the flood. If the heat was sourced by volcanic eruption, acid gas input can lead to acidic flood waters and toxic metal release from the host rock. If the heat source origin was geothermal activity, extensive, long-term fluid–rock interaction would lead to higher pH and less toxic flood waters (Sigvaldason, 1963, 1965; Arnórsson et al., 1983; Steinthórsson and Óskarsson, 1983; Kaasalainen and Stefánsson, 2012). Secondly, the chemical composition of the flood waters is often one of the few, if not the only, indicator of the flood triggering mechanism. As such monitoring of river water chemistry might prove to be an effective method for alerting the public of the possible volcanic eruption in the potential inundated area. Thirdly, glacial floods may play an important role in global cycle of elements. Large number of studies have shown that particulate transport in rivers contribute significantly into the global cycle of elements (e.g. Oelkers et al., 2004, Stefánsdóttir and Gíslason, 2005, Oelkers et al., 2011; Jones et al., 2012a,b; Oelkers et al., 2012). Glacial floods are heavily loaded with suspended material having large surface areas, making it especially reactive once it settles in estuaries. Moreover, suspended particulate flux is far more dependent on runoff than is the dissolved element flux; glacial floods can thus increase dramatically particulate fluxes to the ocean (Gislason et al., 2006). The term 'flux' in this case corresponds to the mass of material transported by water towards the oceans. This particulate material can influence greatly primary productivity along the coast and in lakes (Gislason and Eiriksdottir, 2004).

In this study we focus on the chemical composition of two small Icelandic glacial floods which emerged in July 2011 from the Mýrdalsjökull and the Vatnajökull glaciers. This study was motivated to better understand the origin of the heat source that caused the melting of the glacier and its effect on the flood water chemistry. This study also helps illuminate the potential significance of glacial floods on suspended particulate material transport on a local scale.

2. General description of the study area

2.1. The Mýrdalsjökull glacier and Katla volcanic system

The Mýrdalsjökull glacier is located in southern Iceland within the Eastern Volcanic Zone (Fig. 1a). It covers almost 600 km^2 with a maximum ice thickness of ~740 m in the northern part of the caldera (Björnsson et al., 2000). There is an active central volcano beneath the glacier with a large caldera, which bottom elevation is approximately 650 m above sea level. The caldera, together with an 80 km long northeast-trending fissure swarm, comprises the Katla volcanic system. The circular volcano base is about 30 km in diameter and the highest peaks reach 1380 m above sea level (Björnsson et al., 2000). The caldera is oval shaped with its longest axis trending 14 km NW–SE. The area and volume of ice inside the caldera is 100 km^2 and 45 km^3, respectively. On the caldera rim, the ice cap thickness ranges from 150 to 200 m (Björnsson et al., 2000). Ablation in summer lowers the glacier surface elevation by 4–8 m from spring to autumn. Snow accumulation restores this elevation during the winter. The central volcano is one of the most seismically active in Iceland. The epicentres are usually located within the caldera and beneath the western rim at Goðabunga. Katla erupts roughly twice a century (Larsen, 2000; Óladóttir et al., 2008). It produces high Fe–Ti basalts of the transitional-alkaline magma suite (e.g. Jakobsson, 1979). Katla activity is dominated by explosive subglacial eruptions producing numerous and widespread tephra layers with volumes from ~0.01 to ~1 km^3 (Lacasse et al., 1995; Thordarson and Larsen, 2007; Óladóttir et al., 2008).

The last major glacial flood from Katla occurred in 1918 and was triggered by a volcanic eruption within the caldera with total volume of tephra fallout of 0.7 km^3 (Eggertsson, 1919; Sturkell et al., 2008) and the volume of water-transported material of 0.7–1.6 km^3 (Larsen, 2000). The dense-rock equivalent may have been as high as 1 km^3 (Sturkell et al., 2008). Most of the flood water flowed during an eight-hour period at the initial stages of the eruption. The total flood water volume was estimated to be 8 km^3 (Tómasson, 1996). The majority of the water came from beneath the glacier, breaking the glacial tail. Witnesses reported that large blocks of ice were carried with the flood water. The flood was estimated to have peaked at 300,000 m^3/s and inundated an area of 600–800 km^2 to the east of the volcano (Tómasson, 1996; Larsen, 2000). The coastline moved 4 km towards the sea as the sediments carried by the flood water were deposited. Other smaller glacial floods from Katla, each with a peak discharge of about 2000 m^3/s, occurred in 1955, 1999, and 2011 (Gudmundsson et al., 2013).

2.2. The Vatnajökull glacier and Hamarinn central volcano

The Vatnajökull glacier is the largest in Iceland and covers 8100 km^2. It is situated in the Eastern Volcanic Zone (Fig. 1b). The ice thickness is generally 600–800 m with a maximum thickness of 950 m (Björnsson and Pálsson, 2008). There are several central volcanoes beneath the glacier including the Grímsvötn, Bárðarbunga, Gjálp, and Hamarinn (Gudmundsson and Högnadóttir, 2007). Hamarinn is a central volcano (Fig. 1b) and belongs to the Bárðarbunga–Veidivötn tholeitic volcanic system. This volcanic system is 190 km long and 28 km wide, and it covers an area of 2500 km^2 (Thordarson and Larsen, 2007). Most of the historical eruptions, which account for 14% of the verified eruptions in Iceland, took place on the ice-covered part of the system, forming

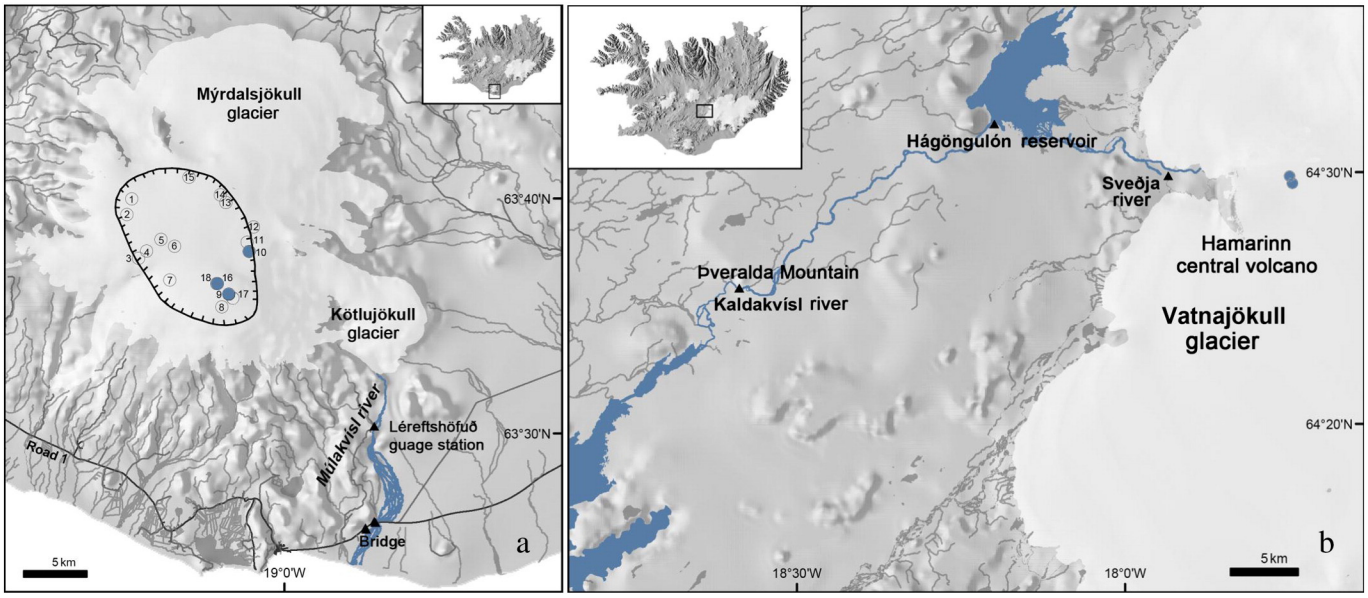

Fig. 1. Location of the sampling sites (black triangles) during the Múlakvísl (a) and Kaldakvísl (b) floods. The blue colour indicates the flood path — see description in the text. The white circles represent the cauldrons existing at the time of writing and the blue circles represent cauldrons which were drained. Hatched line indicates the Katla caldera. The uppermost black triangle on Fig. (a) shows the location of the background sample for the Múlakvísl river and also the location of the gauge station at Léreftshöfuð (see text) (For interpretation of the references to colour in this figure, the reader is referred to the web version of this article.)

small to moderate volumes of basaltic tephra (average magma volume in these eruptions was estimated to be 0.04 km^3 DRE; Thordarson and Larsen, 2007).

A glacial flood originating from the Vatnajökull glacier occurred in November 1996. The eruption which triggered the flood–the Gjálp eruption–produced 0.4 km^3 of magma, making it the fourth largest eruption in Iceland during the twentieth century (Gudmundsson et al., 1997). Melt water accumulated for a month in the Grímsvötn lake prior to its release, when 3.2 km^3 of water drained from the lake within 40 h. The peak discharge was 40,000–50,000 m^3/s (Snorrason et al., 2002; Björnsson, 2003) and most of the water drained into the Skeiðará and Gígjukvísl rivers. The total suspended particulate material flux in the flood water was at least 180 million tonnes (Snorrason et al., 2002; Stefánsdóttir and Gíslason, 2005). This amount is close to 1% of the total annual global river suspended particulates transported to the oceans (Milliman and Syvitski, 1992; Stefánsdóttir and Gíslason, 2005). The dissolved element flux was estimated to be 1 million tonnes, similar to the total annual dissolved load of the largest Icelandic river, the Ölfusá (Gislason et al., 1996; Gislason et al., 2002). The CO_2 flux during the flood was estimated to be 0.6 million tonnes (Gislason et al., 2002). For comparison, the estimated annual average magmatic including geothermal CO_2 flux in Iceland is estimated to be 1–2 millions tonnes (Arnórsson and Gislason, 1994) indicating a major impact of this flood on the annual Icelandic carbon budget.

3. The July 2011 floods

3.1. The Múlakvísl flood

The elevation of most of the Mýrdalsjökull cauldrons, as shown in Fig. 1a, rose by 6–8 m from August 2010 to July 2011, consistent with subglacial water accumulation (Gudmundsson et al., 2013). The greatest rise was measured in cauldron 16 and it equalled 11–12 m (Gudmundsson et al., 2013). Intensified seismicity was observed in the vicinity of the glacier after 2001, possibly caused by magma accumulation under the Katla caldera (IMO, 2013). After 2004, the seismic activity declined until a sudden increase on July 9, 2011 (IMO, 2013). The glacial flood originated from three ice cauldrons in the SE part of the Katla caldera: caldrons 16, 10, and 9, as shown in Fig. 1a (Gudmundsson and Högnadóttir, 2011). The Mýrdalsjökull flood monitoring system of the Icelandic Meteorological Office (IMO, 2013) operates two gauging stations on the Múlakvísl river, which is the main drainage of the Katla glacier (Kötlujökull in Fig. 1a). River monitoring at the Road 1 bridge began to show increased conductivity during the early evening of July 8, around the time of peak seismicity (see Fig. 2b). The increased water level and sediment flux affected the temperature and conductivity sensors around midnight and the sensors were eventually swept away with the bridge few hours later in the early morning of July 9. A photograph of damaged Road 1 and the data recorded by the monitoring station located on the Road 1 bridge can be seen in Fig. 2a and b. Another monitoring station, located at Léreftshöfuð, is normally not in water. Around 4:00 GMT on July 9, it began recording a rising water level, and within minutes the water level rose by more than 5 m. Experience has shown that when the flood peaks at Léreftshöfuð, it reaches Road 1 in about an hour, and may have swept away the bridge on Road 1 at around 5:10 GMT. The exact timing of the beginning of the flood is not known. The seismicity recorded prior to the flood continued, but diminished significantly on July 10 (IMO, 2013).

3.2. The Kaldakvísl flood

Flood water drained from the Hamarinn cauldrons to the Sveðja river and reached the Hágöngulón reservoir on July 13, 2011 (see Fig. 1b). The height of the water level in the Hágöngulón reservoir on July 12 was 816.54 m above sea level and increased to a maximum of 817.33 m above sea level at 12:00 GMT July 13 (Hannesdóttir, 2011). The water discharge filling the reservoir from the Sveðja river increased from 80 m^3/s before midnight on July 12 to 2200 m^3/s at ~3:00 GMT on July 13. The recharge into the reservoir decreased again to ~80 m^3/s at ~18:00 GMT that day. The total volume of the flood water was 20 Gl (Hannesdóttir, 2011). When the water level increased in the Hágöngulón reservoir, water was discharged into the Kaldakvísl river at a rate of ~240 m^3/s. The surface subsidence of the Hamarinn cauldrons was not measured. The seismometer in the vicinity of Hágöngulón detected higher activity around midnight July 13 (IMO, 2013). A similar outburst into the Kaldakvísl river occurred in 1972 with the total volume of 20 Gl (Freysteinsson, 1972).

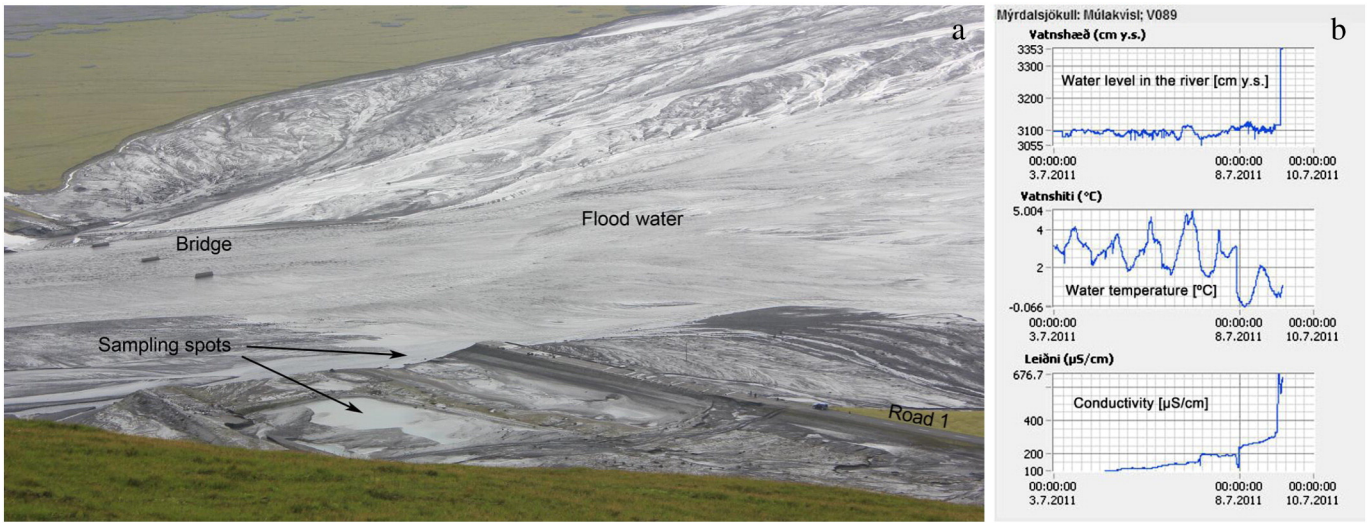

Fig. 2. The Múlakvísl river at the waning stage of the flood. Some of the sampling locations, the remaining parts of the bridge which was swept away by the flood, and Road 1 are highlighted on the photo which was taken on July 10, 2011 at 15:00 GMT. The diagram (b) shows the Icelandic Meteorological Office's continuous monitoring of the water level, temperature and conductivity of the Múlakvísl river which was carried out by the gauge station located on the bridge (IMO, 2013). The plots are stopped at ~5:10 GMT due to the destruction of the monitoring station by the flood.

4. Methods

4.1. Sampling and analyses of flood water and suspended inorganic particulate material

Samples of water and suspended material during the Múlakvísl flood were collected from the Múlakvísl river close to the main bridge on Road 1 and from high standing ponds in the vicinity of the bridge. The high standing ponds represent the chemical composition of the flood water at its highest discharge. The sampling locations are shown in Figs. 1a and 2a, and are described in detail in Table 1. Samples of water and suspended material during the Kaldakvísl flood were collected from (1) the Kaldakvísl river near Þveralda Mountain, (2) from the outlet of the Hágöngulón reservoir, and (3) from the Sveðja river directly at the glacier outlet (Fig. 1b and Table 1). The samples' names during both floods reflect the sampling time. The 'resolution time' is the estimated arrival time of the sampled water at the sampling location. In case of the Múlakvísl flood, the sampling time is the 'resolution time' with exception of the samples collected from high standing points. In these cases, the resolution time refers to that of the flood peak.

There was no significant rainfall during the sampling which could alter the sampled water chemistry. Conductivity and temperature were measured in situ at the time of sampling. Samples were collected in high density polyethylene buckets and poured into 2 L high density polyethylene containers which were sealed after they were filled completely. The buckets and containers were rinsed several times with flood water prior to sampling. Water from the containers was filtered through 0.2 µm Millipore cellulose acetate membranes using a peristaltic pump, silicone tubing, and a 140 mm Sartorius® polypropylene filter holder. At least 1 L of sampled water was pumped through the filtration unit before the samples were collected, and all the air in the unit was expelled through a valve. This filtered sample was divided and stored differently depending on the analysis. Acid washed high density polypropylene bottles were used to collect samples for cations and trace metal analysis. Low and high density polyethylene bottles were used to collect samples for the measurement of other dissolved element concentrations. The containers for dissolved nutrients and dissolved organic carbon analysis were acid washed. During the Kaldakvísl flood, the first samples were collected in plastic 0.5 L Coca- Cola® bottles by a field hydrogeologist present at the site. This was done to maximize sampling during the flood. These bottles were first rinsed several times in hot and cold tap water and then several times with the flood water. These samples were otherwise treated like the other samples. Water samples collected for major and trace element analysis were acidified using Suprapur® 0.5% (v/v) HNO_3. Amber glass bottles were used to collect filtered samples for pH and alkalinity measurements. Samples collected for DOC were acidified with 1.2 M concentrated HCl 2% (v/v).

A variety of methods were used to chemically analyse the sampled flood waters. Dissolved H_2S was measured on site by titration using mercury acetate and dithizone as indicators (Arnórsson, 2000). The pH was determined within 48 h in the laboratory using an Oakton pH electrode. The dissolved inorganic carbon (DIC) was determined from measured pH and alkalinity. The end point of the alkalinity titration was determined by the Gran function. Dissolved F^-, Cl^-, SO_4^{2-}, $S_2O_3^{2-}$, NO_3^-, acetate, and formate concentrations were quantified using an IC-2000 Dionex, ion chromatograph. Cations and trace metals were measured using a Spectro Ciros Vision inductive coupled plasma optical emission spectrometer (ICP-OES), with an in-house standard, and checked against the SPEX Certified Reference Standard. Rare Earth Elements (REE) and some additional trace metals were measured in selected samples using the inductive coupled plasma sector field mass spectrometer ICP-SFMS at ALS Scandinavia, Luleå, Sweden. The dissolved organic carbon (DOC) was measured at Umeå Marine Sciences Centre, Sweden. Analytical measurements had an inter-laboratory reproducibility of within 5.0%.

The inorganic suspended particulate material was collected at the same time as the flood water samples. The remaining unfiltered water sample from the 2 L high density polyethylene containers were shaken vigorously and poured into 1 L high density polyethylene bottles. Water samples containing suspended matter was centrifuged at 15 °C and 9000 rpm, and the recovered solids were freeze-dried for 24 h at −40 °C and 3 PSI pressure. Selected samples of suspended matter were analysed by ICP-OES and ICP-SFMS at ALS Scandinavia, Luleå, Sweden.

During the Múlakvísl flood, ice blocks from the glacier were transported by flood water and spread over an area delimited by the maximum discharge. An ice block sample was collected into a clean heavy walled, low density polyethylene bag and kept frozen. A few days after sampling, the ice sample was melted in the sampling bag. Melted water was filtered through 0.2 µm Millipore cellulose acetate membranes into bottles identical to those used for flood water sampling. Four months after the flood, additional river water sample was taken in the Múlakvísl valley, close to the Léreftshöfuð monitoring station (Fig. 1a).

Table 1
Sample names, location, time of sampling (GMT), temperature, charge imbalance, measured pH, and conductivity at temperature given in the table (T(°C)/pH), T(°C)/conductivity). The charge imbalance was calculated using the PHREEQC computer code at in situ temperatures (Parkhurst and Appelo, 1999).

Sample	Location	GPS	Date	Time Sampling	Time Resolution	Discharge (m^3/s)	Temperature (°C) Air	Water	Charge Imbalance	pH	T(°C) /pH	Conductivity (μS/Cm)	T(°C)/ Conductivity
Múlakvísl													
2011-09-07 0234	West end of bridge over Múlakvísl		7/9/2011	2:34	2:34		7.5		−0.4	7.42	22.5		
2011-09-07 1220	From the west bank of Múlakvísl	63 25 57,6 N 18 52 12,7 W	7/9/2011	12:20	12:20		8.9	3.8	0.6	7.69	22.5	727	4.5
2011-09-07 1350	Pond from the peak discharge	63 26 01,4 N 18 52 16,9 W	7/9/2011	13:50	5:10		8.6	3.7	−0.9	7.77	22	886	5.6
2011-09-07 1625	West end of bridge over Múlakvísl	63 26 15,4 N 18 51 20,1 W	7/9/2011	16:25	16:25		10.5	6.1	0.9	7.79	21.7	352	6
2011-09-07 1725	Highest pond northwest of bridge	63 26 18,3 N 18 51 27,4 W	7/9/2011	17:25	5:10		10.8	3.6	1.6	7.87	22	885	6
2011-09-07 2105	West end of bridge over Múlakvísl	63 26 15,4 N 18 51 20,1 W	7/9/2011	21:05	21:05		9.6	5.6	−10.5	7.95	20.6	180	5.4
2011-10-07 0955	West end of bridge over Múlakvísl	63 26 15,4 N 18 51 20,1 W	7/10/2011	9:55	9:55		9.7	7.1	1.8	7.92	22	172	7
2011-21-11 1400	Background sample	63 30 21,1 N 18 51 26,2 W	11/21/2011	14:00	14:00				0.1	7.56	18.3	144.5	17.8
2011-09-07 2200	Ice block, ca 5 l, close to pond		7/9/2011	22:00					19.7	6.69	13.8		
Kaldakvísl													
2011-13-07 1100	Hágöngulón		7/13/2011	11:00	11:00	240			−5.2	7.69	6.4	107	6.7
2011-13-07 1240	Þveralda		7/13/2011	12:40	4:40	210			2.9	7.55	6.7	108	7.4
2011-13-07 1330	Þveralda		7/13/2011	13:30	5:30	220			2.2	7.58	20.2	117	5.4
2011-13-07 1530	Þveralda		7/13/2011	15:30	7:30	233			−1.0	6.96	20.6	121.1	8.9
2011-13-07 1540	Hágöngulón		7/13/2011	15:40	15:40	240			1.8	6.39	15.7	149.9	6.1
2011-13-07 1630	Þveralda		7/13/2011	16:30	8:30	235			1.9	6.85	20.2	131.1	7.7
2011-13-07 1730	Þveralda		7/13/2011	17:30	9:30	237			1.4	7.16	15.2	136.3	11.4
2011-13-07 1835	Þveralda		7/13/2011	18:35	10:35	240			1.6	6.88	17.9	145.7	7.25
2011-13-07 2015	Þveralda	64 25 44,7 N 18 35 03,9 W	7/13/2011	20:15	12:15	240	8.1	6.4	2.2	8.08	22	135.5	6.2
2011-13-07 2145	Hágöngulón	64 53 59,5 N 18 19 01,8 W	7/13/2011	21:45	21:45	230	7.2		2.2	6.95	21.4	133.3	6
2011-14-07 0055	Þveralda	64 25 44,7 N 18 35 03,9 W	7/14/2011	0:55	16:55	235	5.8	6.2	1.3	8.09	6.2	140	6.1
2011-14-07 0905	Þveralda	64 25 44,7 N 18 35 03,9 W	7/14/2011	9:05	1:05	227	10	6.8	7.1	7.72	9.7	126.5	6.8
2011-14-07 1310	Hágöngulón	64 32 09,6 N 18 11 24,2 W	7/14/2011	13:10	13:10	190	11	6.3	1.4	7.66	22	173.0	6.6
2011-18-07 1900	Sveðja	64 30 N 17 55,4 W	7/18/2011	13:30	13:30	100			1.9	7.27	12.2	151.6	21.9

Table 2
Concentration of dissolved constituents in flood waters measured during the Múlakvísl and Kaldakvísl floods. The DIC concentration was calculated with the PHREEQC computer code (Parkhurst and Appelo, 1999).

Sample	TDS (mg/kg)	DIC (mmol/kg)	Alkalinity (meq/kg)	DOC	Cl	S_2O_3	SO_4	H_2S	Acetate (μmol/kg)	Formate	NO_3	F	B	P	Si	Ca (mmol/kg)	Mg	Na	K	Al	Fe (μmol/kg)	Mn	Sr	As	Ba (nmol/kg)	Br	Co
Múlakvísl																											
2011-09-07 0234	494	5.99	5.57	n.a.	147	16.2	56.1	n.a.	37.2	22.4	2.2	15.5	3.7	0.2	0.347	1.747	0.222	1.750	92.5	0.15	b.d.	6.80	2.73	6.5	11.8	472	1.7
2011-09-07 1220	599	7.11	6.88	n.a.	124	3.6	64.7	0.5	13.9	7.8	2.0	14.8	1.6	0.1	0.267	1.963	0.313	2.556	97.0	0.18	0.21	7.58	3.63	1.5	11.3	b.d	3.3
2011-09-07 1350	807	9.69	9.45	67.4	94.6	10.4	62.3	0.1	25.7	13.1	0.8	20.1	2.4	0.2	0.261	2.066	0.334	4.569	138	0.13	0.11	5.95	5.35	2.0	15.1	b.d	3.4
2011-09-07 1625	240	2.42	2.36	15.0	192	1.2	96.2	0.5	b.d	b.d	2.9	17.5	1.3	0.3	0.176	0.745	0.151	0.960	47.4	2.44	2.35	2.60	1.33	1.7	7.3	725	2.9
2011-09-07 1725	750	8.80	8.67	85.8	93.5	9.8	57.6	1.5	23.3	14.3	0.8	19.2	2.8	0.4	0.271	2.090	0.363	4.115	137	0.15	0.04	6.79	5.33	2.1	16.0	b.d	5.5
2011-09-07 2105	189	1.85	1.83	91.6	201	b.d	107	0.7	b.d	b.d	2.9	17.9	1.1	0.9	0.156	0.457	0.131	0.625	33.0	1.12	0.89	0.74	0.76	1.2	1.8	380	1.0
2011-10-07 0955	151	1.24	1.22	37.5	209	b.d	111	0.5	b.d	b.d	2.7	18.8	1.2	1.0	0.153	0.428	0.134	0.577	31.6	0.43	0.24	0.50	0.66	0.7	1.8	572	0.9
2011-21-11 1400	133	1.22	1.16	31.6	139	b.d	97.4	0.4	b.d	b.d	7.1	24.4	1.5	0.7	0.157	0.333	0.108	0.604	32.8	0.44	0.15	1.58	0.47	n.a.	0.9	184	n.a.
2011-09-07 2200	1.25	0.012	0.008	20.8	1.29	b.d	2.08	0.6	b.d	b.d	b.d	0.18	b.d	b.d	0.001	0.007	0.001	0.004	0.18	0.07	0.07	0.06	0.01	n.a.	b.d	239	n.a.
Kaldakvísl																											
2011-13-07 1100	97.9	0.99	0.94	19.1	45.3	b.d	77.4	1.0	1.10	1.39	b.d	3.69	0.8	0.5	0.072	0.240	0.099	0.338	7.68	1.78	1.23	0.61	0.07	n.a.	n.a.	47.8	n.a.
2011-13-07 1240	88.6	0.84	0.79	35.0	48.7	b.d	74.5	1.5	1.33	1.38	b.d	3.85	0.8	0.6	0.075	0.225	0.110	0.359	8.89	1.72	1.08	0.25	0.07	1.4	0.4	290	1.2
2011-13-07 1330	95.5	0.91	0.86	38.3	47.9	b.d	78.2	0.7	b.d	b.d	b.d	3.93	0.8	0.6	0.077	0.246	0.118	0.379	9.51	0.35	0.05	0.26	0.09	n.a.	n.a.	431	n.a.
2011-13-07 1530	105	1.23	0.99	47.5	45.7	b.d	81.3	0.8	1.46	1.55	b.d	3.74	0.7	0.3	0.081	0.269	0.124	0.382	9.80	0.73	0.57	0.50	0.11	n.a.	n.a.	147	n.a.
2011-13-07 1540	126	2.38	1.19	38.3	57.5	b.d	87.0	0.7	1.02	1.07	b.d	3.61	0.8	0.4	0.084	0.373	0.103	0.508	11.7	0.14	0.85	1.64	0.24	2.7	0.5	76.0	5.8
2011-13-07 1630	108	1.31	1.00	82.4	47.0	b.d	84.0	0.5	1.13	1.61	b.d	3.71	0.8	0.2	0.082	0.295	0.119	0.419	10.3	0.33	0.33	0.72	0.13	n.a.	n.a.	220	n.a.
2011-13-07 1730	114	1.25	1.07	97.4	48.6	b.d	84.7	0.4	b.d	b.d	1.4	4.06	0.8	0.4	0.085	0.311	0.115	0.466	10.7	0.16	0.05	0.66	0.15	n.a.	n.a.	229	n.a.
2011-13-07 1835	120	1.48	1.13	85.8	46.9	b.d	88.6	0.5	1.21	1.64	b.d	3.85	0.8	0.2	0.086	0.336	0.117	0.485	11.4	0.39	0.35	0.90	0.17	n.a.	n.a.	10.5	n.a.
2011-13-07 2015	119	1.12	1.12	33.3	48.4	b.d	84.8	0.5	1.94	b.d	b.d	4.20	0.8	0.4	0.084	0.326	0.113	0.505	11.5	0.76	0.34	0.45	0.18	3.0	0.5	b.d	0.6
2011-13-07 2145	111	1.29	1.04	44.1	52.3	b.d	80.2	0.5	b.d	b.d	b.d	3.95	0.8	0.0	0.079	0.303	0.107	0.474	11.8	0.13	0.16	0.91	0.19	n.a.	n.a.	309	n.a.
2011-14-07 0055	118	1.14	1.12	60.8	51.9	b.d	82.8	0.7	1.28	b.d	b.d	4.29	1.1	0.5	0.083	0.311	0.112	0.521	10.5	0.52	0.14	0.42	0.18	2.8	0.5	b.d	0.7
2011-14-07 0905	98.3	0.91	0.87	20.0	53.4	b.d	70.1	0.5	b.d	b.d	b.d	4.25	0.8	0.5	0.079	0.262	0.115	0.470	9.30	0.46	0.05	0.31	0.13	2.4	0.7	549	0.7
2011-14-07 1310	137	1.40	1.34	42.5	51.0	b.d	84.6	0.6	1.32	1.61	b.d	4.13	0.9	0.4	0.087	0.377	0.121	0.597	12.0	0.47	0.21	0.74	0.28	3.5	1.2	70.1	1.1
2011-18-07 1900	113	1.36	1.20	40.8	16.5	2.1	48.1	0.6	5.04	2.53	1.4	2.72	0.5	0.3	0.068	0.446	0.088	0.278	9.65	1.78	1.45	2.04	0.19	1.9	1.2	327	3.6

n.a. = not analysed; b.d. = below detection limit.
Values marked with the shadowed background are below accreditation limit of the ALS Scandinavia Laboratory.

Table 2 (*continued*)

Sample	Cr	Cu	Sb	Ti	V	W	Cd	Hg	Mo	Ni	Pb	Zn	Th	La	Ce	Pr	Nd	Sm	Eu	Gd	Tb	Dy	Ho	Er	Tm	Yb	Lu
															(nmol/kg)												
Múlakvísl																											
2011-09-07 0234	1.4	16.2	39.8	2.4	122.3	b.d	0.1	b.d	9.1	20.8	0.2	60.8	b.d.	0.007	0.010	0.002	0.005	0.001	0.001	0.003	0.001	0.005	0.001	0.003	0.001	0.005	0.002
2011-09-07 1220	b.d.	3.9	b.d	19.3	49.5	13.5	0.1	b.d	10.9	13.8	0.1	12.9	b.d.	0.040	0.062	0.008	0.038	0.008	0.002	0.010	0.001	0.010	0.002	0.011	0.001	0.011	0.004
2011-09-07 1350	0.4	2.3	b.d	28.4	58.3	18.9	0.1	0.0	20.8	17.0	0.2	6.4	b.d.	0.061	0.106	0.015	0.062	0.014	0.009	0.009	0.002	0.013	0.004	0.012	0.002	0.016	0.004
2011-09-07 1625	0.9	5.5	b.d	724.9	84.2	27.6	0.1	b.d	9.2	7.7	0.2	26.0	b.d.	0.652	1.492	0.202	0.756	0.157	0.045	0.099	0.015	0.086	0.016	0.043	0.004	0.029	0.007
2011-09-07 1725	b.d.	8.1	b.d	401.1	64.4	17.5	0.0	b.d	18.2	22.0	0.2	63.8	b.d.	0.395	0.821	0.113	0.440	0.082	0.025	0.054	0.009	0.058	0.010	0.030	0.005	0.025	0.005
2011-09-07 2105	0.5	3.3	b.d	137.9	116.6	33.2	b.d.	b.d	8.7	4.9	0.1	13.0	b.d.	0.086	0.198	0.027	0.116	0.026	0.005	0.014	0.002	0.012	0.002	0.007	0.001	0.005	0.001
2011-10-07 0955	b.d.	2.6	b.d	71.2	126.2	32.0	0.0	b.d	8.8	4.0	0.1	3.9	b.d.	0.068	0.131	0.018	0.073	0.021	0.005	0.010	0.002	0.012	0.001	0.004	0.000	0.002	0.001
2011-21-11 1400	n.a.	n.a.	b.d	31.9	72.4	b.d	n.a.	n.a.	n.a.	n.a.	n.a.	n.a.	n.a.	n.a.	n.a.	n.a.	n.a.	n.a.	n.a.	n.a.	n.a.	n.a.	n.a.	n.a.	n.a.	n.a.	n.a.
2011-09-07 2200	5.4	n.a.	30.2	10.0	28.3	b.d	n.a.	n.a.	n.a.	n.a.	n.a.	n.a.	n.a.	n.a.	n.a.	n.a.	n.a.	n.a.	n.a.	n.a.	n.a.	n.a.	n.a.	n.a.	n.a.	n.a.	n.a.
Kaldakvísl																											
2011-13-07 1100	n.a.	n.a.	b.d	285.4	80.9	36.3	n.a.	n.a.	n.a.	n.a.	n.a.	n.a.	n.a.	n.a.	n.a.	n.a.	n.a.	n.a.	n.a.	n.a.	n.a.	n.a.	n.a.	n.a.	n.a.	n.a.	n.a.
2011-13-07 1240	1.8	6.9	b.d	161.9	98.0	b.d	b.d.	b.d	2.6	4.4	0.1	24.3	b.d.	0.071	0.153	0.026	0.087	0.028	0.009	0.016	0.004	0.017	0.004	0.011	0.002	0.010	0.002
2011-13-07 1330	n.a.	n.a.	b.d	12.7	124.7	b.d	n.a.	n.a.	n.a.	n.a.	n.a.	n.a.	n.a.	n.a.	n.a.	n.a.	n.a.	n.a.	n.a.	n.a.	n.a.	n.a.	n.a.	n.a.	n.a.	n.a.	n.a.
2011-13-07 1530	n.a.	n.a.	4.6	80.2	95.2	49.1	n.a.	n.a.	n.a.	n.a.	n.a.	n.a.	n.a.	n.a.	n.a.	n.a.	n.a.	n.a.	n.a.	n.a.	n.a.	n.a.	n.a.	n.a.	n.a.	n.a.	n.a.
2011-13-07 1540	n.a.	5.4	b.d	26.1	76.6	35.9	0.0	b.d	2.9	10.8	0.1	15.2	b.d.	0.019	0.036	0.008	0.026	0.005	0.003	0.003	0.001	0.004	0.001	0.002	0.001	0.004	0.001
2011-13-07 1630	n.a.	n.a.	b.d	42.0	95.0	5.4	n.a.	n.a.	n.a.	n.a.	n.a.	n.a.	n.a.	n.a.	n.a.	n.a.	n.a.	n.a.	n.a.	n.a.	n.a.	n.a.	n.a.	n.a.	n.a.	n.a.	n.a.
2011-13-07 1730	n.a.	n.a.	40.0	10.2	126.2	12.0	n.a.	n.a.	n.a.	n.a.	n.a.	n.a.	n.a.	n.a.	n.a.	n.a.	n.a.	n.a.	n.a.	n.a.	n.a.	n.a.	n.a.	n.a.	n.a.	n.a.	n.a.
2011-13-07 1835	n.a.	n.a.	b.d	67.3	124.3	11.9	n.a.	n.a.	n.a.	n.a.	n.a.	n.a.	n.a.	n.a.	n.a.	n.a.	n.a.	n.a.	n.a.	n.a.	n.a.	n.a.	n.a.	n.a.	n.a.	n.a.	n.a.
2011-13-07 2015	0.6	6.4	7.3	65.4	93.2	45.0	0.0	b.d	2.9	4.4	0.1	27.4	b.d.	0.030	0.056	0.010	0.038	0.010	0.002	0.008	0.002	0.006	0.002	0.004	0.001	0.004	0.002
2011-13-07 2145	n.a.	n.a.	36.9	14.4	94.2	b.d	n.a.	n.a.	n.a.	n.a.	n.a.	n.a.	n.a.	n.a.	n.a.	n.a.	n.a.	n.a.	n.a.	n.a.	n.a.	n.a.	n.a.	n.a.	n.a.	n.a.	n.a.
2011-14-07 0055	2.0	6.2	21.8	72.9	97.2	22.4	0.0	b.d	3.0	5.1	0.1	181.9	b.d.	0.026	0.056	0.008	0.035	0.010	0.003	0.008	0.001	0.009	0.002	0.006	0.000	0.004	0.005
2011-14-07 0905	n.a.	4.3	b.d	76.9	110.5	20.5	0.0	b.d	3.1	3.5	0.1	15.4	b.d.	0.031	0.071	0.009	0.046	0.010	0.001	0.006	0.001	0.007	0.001	0.003	0.000	0.004	0.002
2011-14-07 1310	2.7	7.9	b.d	80.4	90.9	28.2	0.1	b.d	3.3	6.8	0.2	98.9	b.d.	0.044	0.091	0.013	0.065	0.013	0.005	0.010	0.002	0.008	0.002	0.006	0.001	0.005	0.002
2011-18-07 1900	1.9	5.1	b.d	468.0	65.2	55.9	b.d.	b.d	1.4	9.2	0.1	20.5	b.d.	0.207	0.475	0.065	0.297	0.065	0.025	0.046	0.009	0.053	0.011	0.028	0.004	0.026	0.005

n.a. = not analysed; b.d. = below detection limit.

Values marked with the shadowed background are below accreditation limit of the ALS Scandinavia Laboratory.

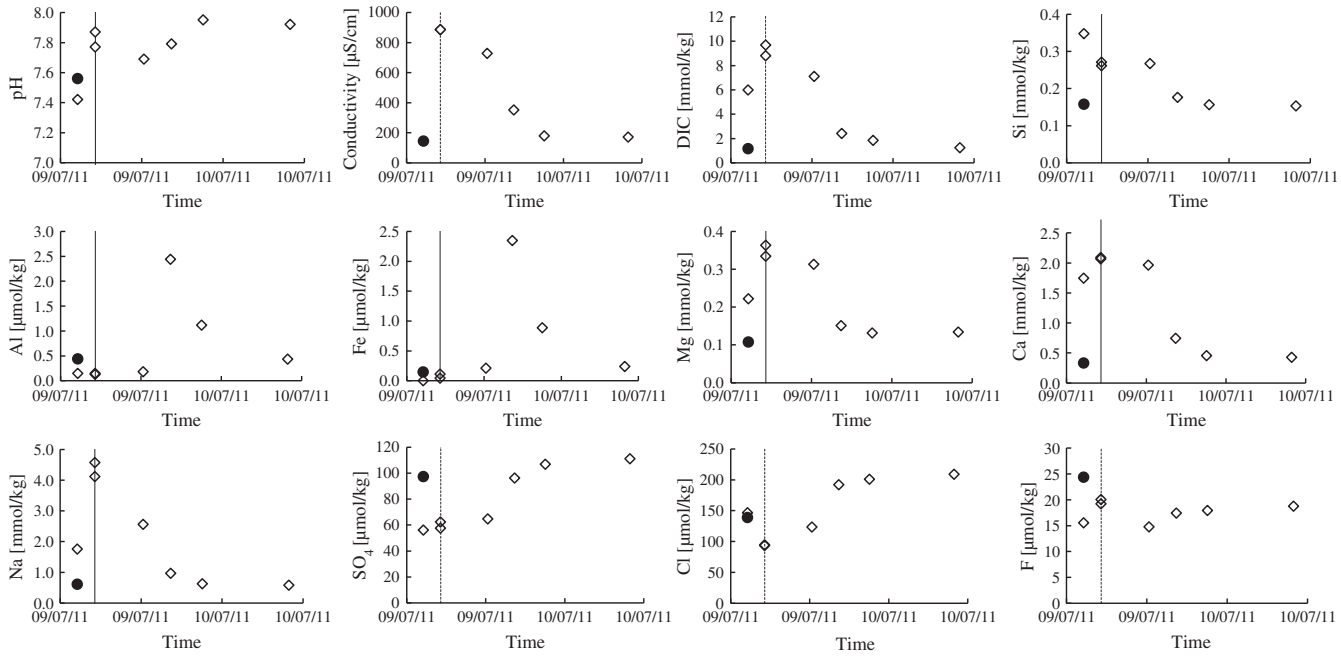

Fig. 3. The pH, conductivity and dissolved constituent concentrations in the sampled water during the Múlakvísl flood. The filled circles represent the element concentrations in the sample obtained four months after the flood. It reflects the background chemical composition of the Múlakvísl river. The vertical line represents the peak of the flood.

4.2. Discharge measurements and dissolved element fluxes calculations

Water discharge during the Múlakvísl flood was estimated by the Icelandic Meteorological Office using the HEC-RAS model which included the cross section and the height of the water table in the flood channel (Brunner, 2010; Jónsson and Þórarinsdóttir, 2011). The water velocity was 3–4 m/s and the average discharge was ~2500 m^3/s. The total discharge during the flood peak, between 4 and 6:30 GMT on July 9, was 7–8 Gl at Léreftshöfuð (Jónsson and Þórarinsdóttir, 2011). The total volume of water released from the cauldrons, based on ice cap surface measurements before and after the flood, was estimated to be 18 Gl (Gudmundsson and Högnadóttir, 2011). Based on this assessment, it is estimated that 10 Gl of flood water was discharged after the flood peak, as 'post-peak discharge'. Total major dissolved element fluxes (Si, Ca, Mg, Na, K, Al, Fe, Mn, Sr, Cl, SO_4, F, DIC) were calculated from measured sample water element concentrations (Table 2) and the total discharge (Gudmundsson and Högnadóttir, 2011). The total dissolved element fluxes carried by the flood waters were a combination of background fluxes, dissolved fluxes during the flood peak, and dissolved fluxes during the rest of the flood. The dissolved element fluxes during the flood peak were estimated by multiplying the average element concentrations of the first four samples (samples: 2011-09-07_0234; 2011-

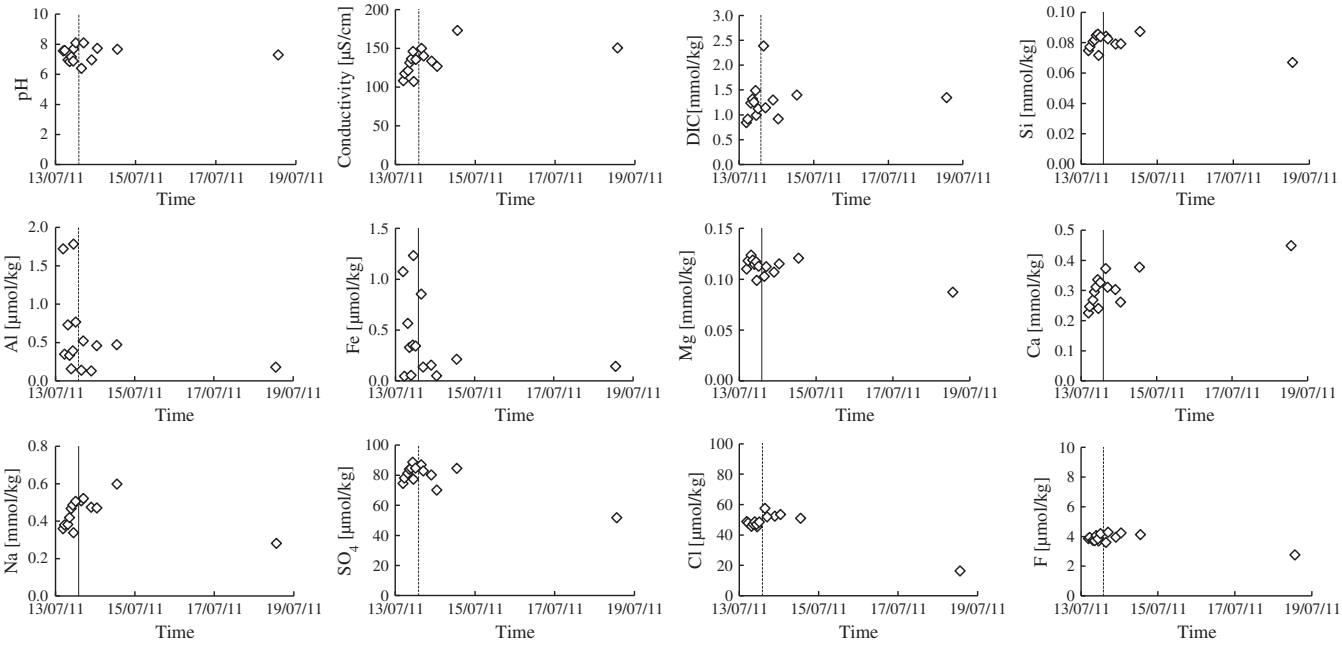

Fig. 4. The pH, conductivity and dissolved constituent concentrations in the sampled water during the Kaldakvísl flood. The last sample, taken on July18, 2011, represents the chemical composition of the undiluted water collected directly at the Vatnajökull glacier outlet from the Sveðja river. The other samples represent the chemical composition of the mixture of flood water and water from the Hágöngulón reservoir before flood started (Fig. 1b). The vertical line represents the flood peak.

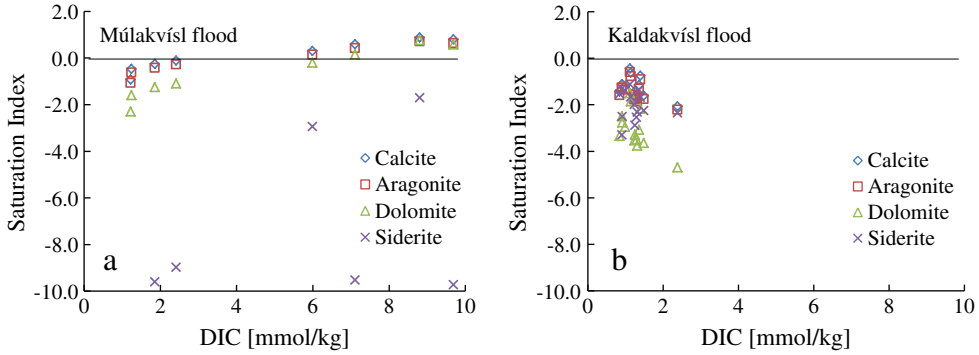

Fig. 5. The saturation state of the sampled water with respect to carbonates during Múlakvísl (a) and Kaldakvísl flood (b). Samples taken during the first hours of the Múlakvísl flood were supersaturated with respect to carbonate minerals in contrast with the Kaldakvísl flood water which was undersaturated with respect to carbonates.

09-07_1220; 2011-09-07_1350; 2011-09-07_1725) by the total flood peak discharge of 8 Gl (Gudmundsson and Högnadóttir, 2011; Jónsson and Þórarinsdóttir, 2011). The dissolved element fluxes during the rest of the flood were estimated by multiplying the average elemental concentrations of other three samples (samples: 2011-09-07_1625; 2011-09-07_2105; 2011-10-07_0955) by the post-peak discharge of 10 Gl (Gudmundsson and Högnadóttir, 2011; Jónsson and Þórarinsdóttir, 2011). The background element fluxes were estimated by multiplying the major element concentrations of the sample taken 3.5 months after the flood from the Múlakvísl river (sample 2011-21-11_1400) by the average discharge measured in Múlakvísl river in July 1998 (Kristmannsdóttir et al., 2006). The 1998 July discharge was used in this calculation due to the lack of more recent July Múlakvísl river discharge data. The effect of the flood on dissolved element fluxes was determined by subtracting the background element fluxes from the total dissolved fluxes during the entire flood.

The water discharge during the Kaldakvísl flood was measured directly at the Landsvirkjun Power Company monitoring station located at the Hágöngulón reservoir. The average flood water discharge from the Hágöngulón reservoir into the Kaldakvísl river was 240 m^3/s (Table 1). The total discharge into the Hágöngulón during the flood was estimated to be 30 Gl, of which around 20 Gl were assigned to the glacial flood and 10 Gl were assigned to other sources recharging the reservoir (Hannesdóttir, 2011). The total dissolved element fluxes were calculated by multiplying the average elemental concentrations of sampled waters by the discharge of 30 Gl. To estimate the background element fluxes — the average major elemental concentrations measured in Sveðja river in 1994 (Hjartarson, 1994) were multiplied by the discharge of 10 Gl. As was the case for the Múlakvísl river, July 1994 discharge data was used due to the lack of more recent data. The effect of the flood on element fluxes was determined by subtracting the background element fluxes from the total dissolved element fluxes during the entire flood.

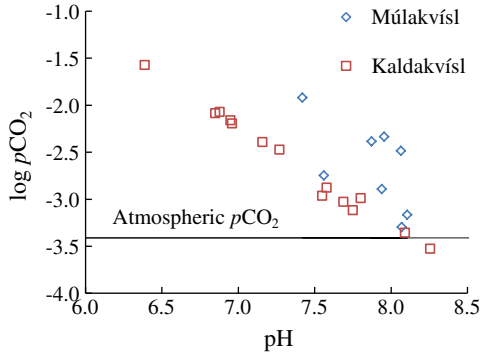

Fig. 6. The logarithm of the *in situ* partial pressure of CO_2 (pCO_2) of the sampled waters versus *in situ* pH. The horizontal line represents the logarithm of CO_2 partial pressure (pCO_2) in the atmosphere.

4.3. Saturation state and dissolution rate calculations

The standard state adopted in this study is unit activity for pure minerals and H_2O at any temperature and pressure. The standard state for aqueous species is a hypothetical 1 molal solution referenced to infinite dilution at any temperature and pressure. Aqueous speciation, charge imbalance, and mineral saturation states were calculated using the PHREEQC 2.17 geochemical code (Parkhurst and Appelo, 1999) with the standard *phreeqc.dat* database updated with selected aqueous complex formation and mineral solubility constants taken from Gysi and Stefánsson (2011) and using measured water sample compositions, pH, and temperature. The thermodynamic properties of the hydrated Katla and Grímsvötn glass surfaces were estimated from the stoichiometrically weighted sum of the hydrolysis reactions of amorphous SiO_2 and amorphous $Al(OH)_3$ (Bourcier et al., 1990; Wolff-Boenisch et al., 2004). The equilibrium constants of individual hydrolysis reactions required for this estimation were taken from *phreeqc.dat*. The logarithm of the equilibrium constant for the hydrated basaltic glass surface hydrolysis reaction:

$$Si_{1.0}Al_{0.32}O_2(OH)_{0.96} + 0.96H^+ + 1.04H_2O = 0.32Al^{3+} + H_4SiO_4, \quad (1)$$

was calculated to be 0.76 for both glasses at 25 °C. The saturation state of the flood waters with respect to the hydrated glasses is reported as the Gibbs free energy of reaction, ΔG_r, but the saturation state of the flood waters with respect to secondary minerals is reported as the saturation index, SI. The relationship between these parameters is given by:

$$\Delta G_r = RT2.303 \ \log \ (Q/K) = RT2.303 \ SI \quad (2)$$

where R (J/K/mol) corresponds to the gas constant, T designates the temperature in Kelvin, Q stands for the reaction quotient (also called ion activity product), and K denotes the equilibrium constant of the relevant reaction at the temperature of interest. Both ΔG_r and SI are zero at equilibrium and negative when the fluid is undersaturated with respect to the solid.

The far-from-equilibrium dissolution rate of basaltic glass can be described using (Oelkers and Gislason, 2001)

$$r_{+,BET} = k\left(\frac{a_{H^+}^3}{a_{Al^{3+}}}\right)^{0.35} \quad (3)$$

where r_{+BET} signifies the BET (Brunauer–Emmett–Teller; Brunauer et al., 1938) surface area normalized far from equilibrium steady-state dissolution rate, k refers to a rate constant equal to $10^{-11.65}$ mol of $Si/cm^2/s$, and a_i represents the activity of subscripted aqueous species. Note that hydrated basaltic glass dissolution rates slow down when equilibrium is approached (c.f. Oelkers and Gislason, 2001). This effect, however, is only substantial when ΔG_r exceeds −10 kJ/mol at 25 °C, and is thus negligible in this study.

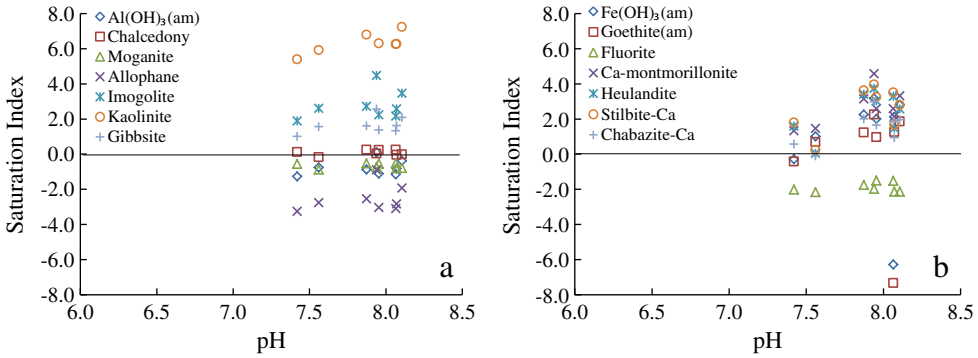

Fig. 7. The *in situ* pH dependence of the saturation state of sampled waters with respect to selected secondary minerals during Múlakvísl flood depicted in terms of saturation index.

Reaction path modelling with the aid of PHREEQC 2.17 was used to evaluate the possible origin of the dissolved constituents in the Múlakvísl flood water. The aim of the modelling was to match modelling results of water–basalt interaction with measured flood water chemistry. The modelling was performed assuming either reduced or oxidized conditions. The redox conditions in reduced system was set by Fe^{2+}/Fe^{3+} equilibrium due to the composition of the dissolving basalt and precipitating goethite/siderite. The redox conditions in the oxidized system were set by assuming the flood water was in equilibrium with atmospheric O_2. The initial fluid used in the model was pure water, since the water originated from melted ice was very dilute, with total dissolved solids (TDS) of 1.3 mg/kg (Table 1), to which CO_2 gas was added until the concentration of the dissolved gas corresponded to the highest measured DIC in the water samples collected during the Múlakvísl flood; in total 9 mmol/kg, was added. Due to low concentration of H_2S measured in the sampled waters, this gas was not included in the calculations. Other gases: SO_2, HF, and HCl were not included in the initial fluid since their concentrations were within that commonly measured in Múlakvísl river (Kristmannsdóttir et al., 2006). The fluid was allowed to react incrementally with Katla basalt (Óladóttir et al., 2008), and secondary minerals were allowed to precipitate at local equilibrium. Secondary phases were chosen based on natural analogues and the saturation state of sampled flood waters with respect to secondary minerals. Results are plotted in this study as functions of the mass of basalt dissolved into each kg of water.

5. Results

5.1. Flood water chemistry

5.1.1. Múlakvísl flood

The results of chemical analysis of the Múlakvísl flood samples are shown in Tables 1 and 2, Fig. 3 and Fig. 1 in Electronic supplement. The average charge imbalance of the analysed samples was −0.9%, and most was within 2%. The highest charge imbalance was calculated for sample 2011-10-07_0955 and it equalled −10.5%. The charge imbalance for the melted ice (2011-09-07_2200) equalled 19.7%, which is not unusual for waters with very low total dissolved solids (in this case the TDS equalled 1.3 mg/kg), mostly due to uncertainties in the alkalinity titration measurements. The average measured flood water temperature was 5 °C whereas the average measured air temperature at the time of sampling was 9.4 °C. The highest measured conductivity was in the pond water, which represents the flood peak, equalled ~890 μS/cm. The pH of the samples was between 7.4 and 8. The concentration of all elements other than SO_4^{2-}, Cl, and F increased during the flood compared to the post-flood background sample and river monitoring in 1997 and 1998 (Kristmannsdóttir et al., 2006).

The average dissolved H_2S concentration in the sampled waters was 0.6 μmol/kg–close to the analytical detection limit. There was no characteristic H_2S smell; however, there was an unidentified smell in the air. The gas sensors detected neither H_2S nor SO_2 in the air at the sampling site, but traces of CO (5–6 ppm) were detected in the air at the Léreftshöfuð site. Dissolved $S_2O_3^{2-}$, acetate, and formate concentrations in the water samples were the highest at the beginning of the flood (16, 37.2, and 22.3 μmol/kg, respectively) and decreased gradually to zero with time. The highest DIC, F, and B concentrations were also measured at the beginning of the flood (during the flood peak) and equalled 9.7 mmol/kg, 20 μmol/kg, and 3.7 μmol/kg, respectively. Conversely, SO_4, Cl, and P concentrations maximized at the end of the flood and their maximum concentrations were 111, 209, and 1.0 μmol/kg, respectively (Table 2). The highest concentrations of the major dissolved elements Si, Mg, Ca, Na, and K were observed during the first few hours of the flood. Similar trends were observed for some of the trace element concentrations including Sr, Co, Cu, Ni, Zn, Mo, and As. The concentrations of Al, Fe, and Ti increased continuously up to 14 h after the flood peak. The highest REE concentrations in collected waters from the Múlakvísl flood were measured in sample 2011-09-07_1655-almost 12 h after the flood peak reached the bridge. Similar trends were observed for Al, Fe, and Ti-the highest concentrations were measured in this sample.

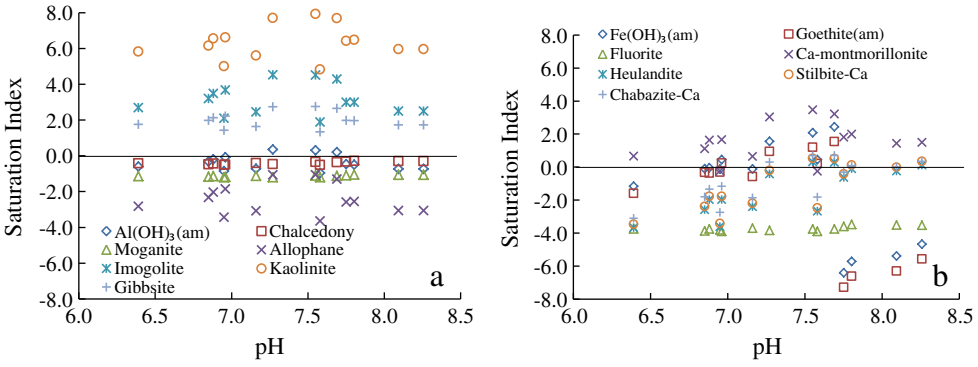

Fig. 8. The *in situ* pH dependence of the saturation state of sampled waters with respect to selected secondary minerals during Kaldakvísl flood depicted in terms of saturation index.

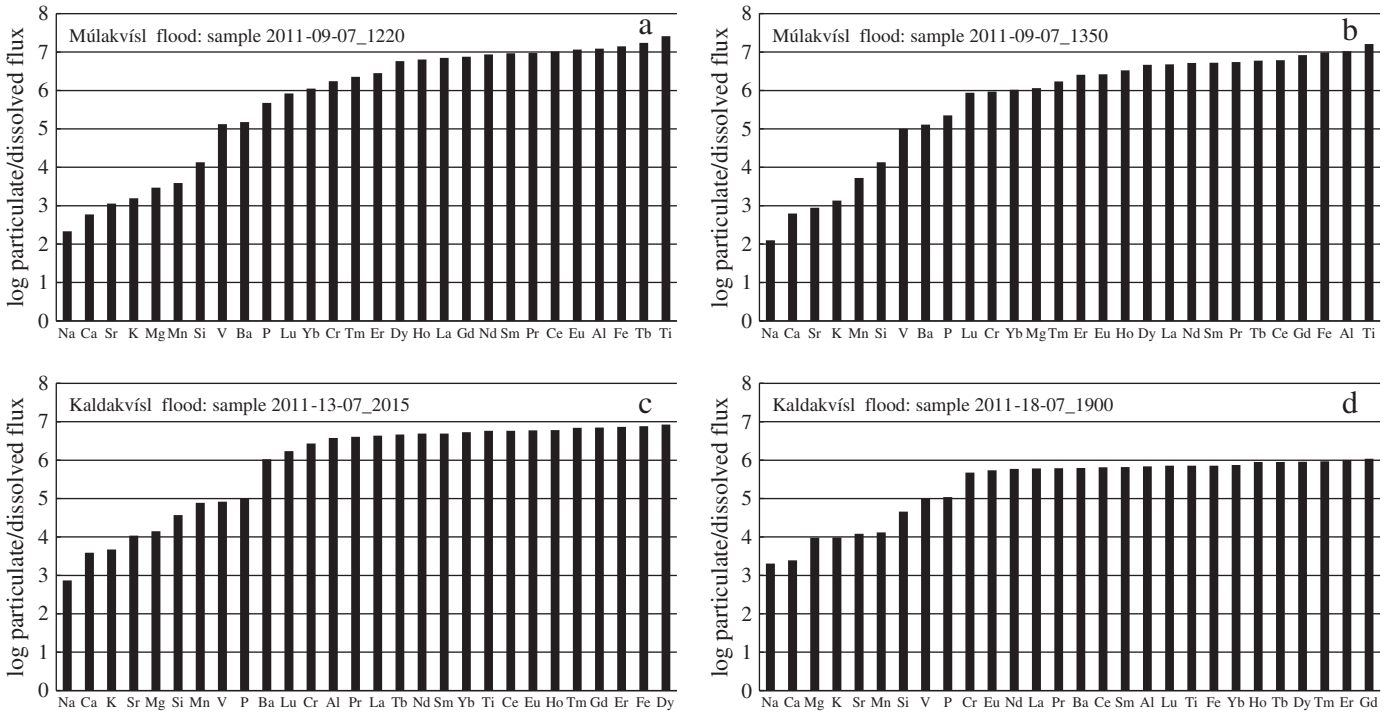

Fig. 9. The logarithm of the ratio of particulate flux to dissolved flux of selected elements in the Múlakvísl (a, b) and Kaldakvísl flood waters (c, d).

According to the saturation state calculations, the flood water samples were supersaturated with respect to the carbonates including calcite, aragonite, and dolomite at the beginning of the flood, when the DIC concentration was > 6 mmol/kg (Fig. 5a). The partial pressure of CO_2 in sampled flood water was higher than atmospheric indicating its degassing (Fig. 6). The flood waters were supersaturated with respect to the less soluble Al-bearing secondary phases including gibbsite imogolite, kaolinite, Ca-montmorillonite and zeolites (stilbite, heulandite, and chabazite) (Fig. 7a and b). Flood waters were undersaturated with respect to siderite, $Al(OH)_{3(am)}$, moganite, allophane, and fluorite, but close to saturation with respect to chalcedony. All the flood water samples but one were supersaturated with respect to goethite and amorphous $Fe(OH)_3$.

5.1.2. Kaldakvísl flood

The results of chemical analysis of the Kaldakvísl flood samples are shown in Tables 1 and 2, Fig. 4 and Fig. 2 in Electronic supplement. The average charge imbalance of the analysed samples was 1.54% and most was within 3%. The average measured flood water temperature was 6.4 °C whereas the average measured air temperature was 8.4 °C. A maximum conductivity of 173 μS/cm was measured in the Hágöngulón, 26 h after the flood started (sample 2011-14-07_1310) and it did not correlate with the flood peak. The measured flood water pH was between 6.4 and 8.1. The concentrations of most elements increased with time during the flood.

The average H_2S concentration of the flood water was 0.7 μmol/kg, close to the analytical detection limit. The $S_2O_3^{2-}$ concentration in the flood waters was below the detection limit of 0.1 μmol/kg with exception of the sample collected from the Sveðja river five days after the flood started (sample: 2011-18-07_1900). The concentration of acetate and formate was also the highest in this sample (Table 2). Similar to the Múlakvísl flood, the partial pressure of CO_2 in the flood water was higher than atmospheric leading to its degassing. There

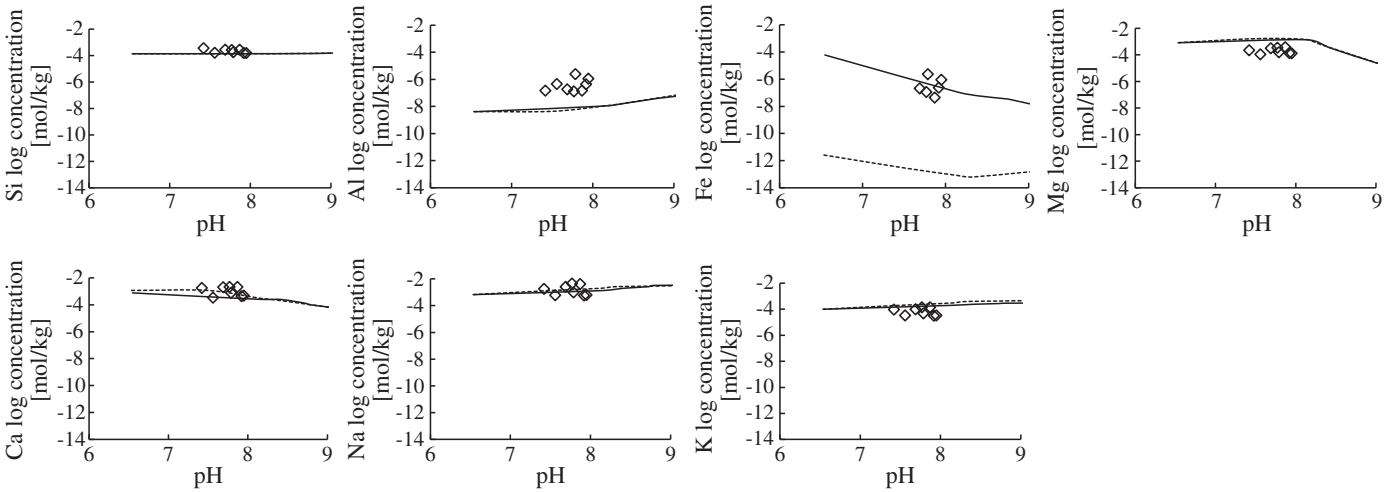

Fig. 10. A comparison of the concentrations of major elements in the Múlakvísl flood water (open diamonds) with those obtained by reaction path modelling (solid curves) versus *in situ* pH. The dotted curves on the plots represent modelled concentrations assuming oxidized conditions whereas solid curves show modelled concentrations assuming reducing conditions.

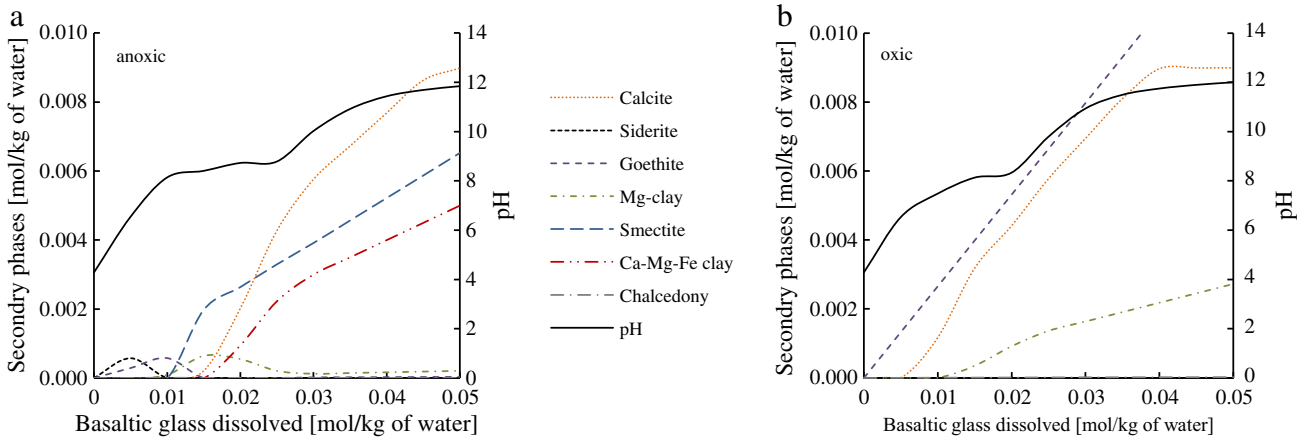

Fig. 11. Results of the reaction path modelling where basaltic glass was allowed to dissolve in a closed system and secondary phases were precipitating at local equilibrium. Plot (a) presents the mass of secondary phases precipitated in anoxic conditions whereas plot (b) shows the mass of secondary phases precipitated in oxic conditions.

was an undefined odour noticed at the Hágöngulón reservoir. The measured concentrations of most of the elements including DIC, Si, Mg, Ca, Na, SO_4, K, Mn, Sr, B, Co, Ni, and Zn increased with time during the first 12 h of the flood. Concentrations subsequently decreased until the last sample, which was taken 26 h after the flood started (2011-14-07_1310) when they again increased. The Al, Fe, Ti, V, and H_2S concentrations showed a different pattern with the highest concentrations at the beginning of the flood. Concentrations of the trace metals As, Cr, Cu, Cd, Mo and Pb were the highest in the last sample collected on July 14 (2011-14-07_1310). The REE concentrations were the highest in the sample taken closest to the source of the flood in Sveðja, five days after the flood started (2011-18-07_1900). In contrast with the Múlakvísl flood, where Al, Fe, and Ti concentrations correlated with REE, there was no correlation between REE and Al, Fe, and Ti concentrations in the Kaldakvísl flood water samples. Moreover, there was no correlation between REE concentrations and the other measured elements.

According to saturation state calculations, all flood water samples were undersaturated with respect to the carbonates including calcite, aragonite, dolomite, and siderite (Fig. 5b). The partial pressure of CO_2 in sampled water was higher than atmospheric indicating its degassing (Fig. 6). Water was supersaturated with respect to the less soluble Al-bearing secondary phases including gibbsite, imogolite, kaolinite and Ca-montmorillonite (Fig. 8a and b). Flood water samples were supersaturated with respect to the zeolites: stilbite, heulandite, and chabazite during first several hours of the flood. Samples were mostly undersaturated with respect to chalcedony, moganite, allophane, and amorphous $Al(OH)_3$. Samples taken within first several hours of the flood and the sample taken 5 days after the flood in Sveðja were supersaturated with respect to goethite and amorphous $Fe(OH)_3$.

5.2. Dissolved element fluxes and particulate material transport

The total dissolved fluxes carried by the flood water in the Múlakvísl river were estimated to be 5100 tonnes, and the total dissolved fluxes carried by the flood water in the Kaldakvísl river were estimated to be 2300 tonnes. For comparison, the annual dissolved fluxes carried by the Ölfusa river, the biggest river in Iceland is estimated to be 0.8 million tonnes/year (Eiriksdottir et al., 2012b).

Total flux of CO_2, mainly in form of dissolved bicarbonate (HCO_3^-) during the Múlakvísl and Kaldakvísl floods were 3300 and 1400 tonnes, respectively. For comparison, the annual magmatic flux of CO_2 into the atmosphere and surface waters in Iceland, originated mostly from the long-term degassing of volcanoes and geothermal systems, has been estimated to be 1–2 tonnes (Arnórsson and Gislason, 1994). According to Gislason et al. (1996), the annual transient fixation of atmospheric CO_2 by chemical weathering in Iceland is 3.3 million tonnes and the annual permanent CO_2 fixation by potential carbonate precipitation in the ocean, resulting from the dissolved riverine Ca and Mg fluxes from Iceland is 900,000 tonnes.

The effect of glacial floods on particulate material transport is far greater than that of the dissolved transport. Due to high discharge during the floods, flood waters can carry greater amounts of particulates increasing the suspended load. This is evident in the samples collected in this study. For example, the suspended material concentration in sample 2011-09-07_1220, collected 7 h after the flood peak in Múlakvísl was 47 g/L whereas this concentration in sample 2011-10-07_0955, collected 29 h after the flood peak, was only 30 mg/L. This latter concentration is within the range typically measured in Icelandic rivers (Pálsson and Vigfusson, 1996; Eiriksdottir, 2007; Eiriksdottir et al., 2011, 2012a, 2013b). The ratio of particulate to the dissolved flux for various elements in the flood waters was calculated for four samples, for which suspended particulate material was collected and its chemical composition was measured; the results of these calculations are shown in Fig. 9. These ratios were calculated by dividing the measured particulate element concentrations by the corresponding dissolved element concentrations. The element most abundant in dissolved form was Na followed by Ca, Sr, Mn, Mg, K, and Si. The elements most transported by the particulates were Fe, Ti, Al, and REE. Note that that the concentrations of C, S, Cl, F, B, As, and Mo were not measured in the suspended material.

6. Discussion

6.1. Chemical trends in the flood waters and comparison of their compositions with typical Icelandic surface- and groundwaters

Water samples collected during both floods were neutral to alkaline (pH 7–8) and enriched in DIC; as shown in Table 2, the DIC of the Múlakvísl and Kaldakvísl flood waters were as high as 9.7 and 2.4 mmol/kg, respectively, implying extensive water rock interaction (Gislason and Eugster, 1987; Gislason et al., 1996, 2009; Oskarsdottir et al., 2011; Galeczka et al., 2014). The typical DIC concentration of Icelandic river waters is less than 2 mmol/kg, (Gislason et al., 1996; Eiriksdottir, 2007; Louvat et al., 2008; Pogge von Strandmann et al., 2008; Vigier et al., 2009; Oskarsdottir et al., 2011) but some surface geothermal waters can have DIC as high as 8 mmol/kg (Arnórsson et al., 1983; Kaasalainen and Stefánsson, 2012). The background DIC concentration in the Múlakvísl river measured in the summers of 1997 and 1998 ranged between 0.7 and 2.7 mmol/kg (Kristmannsdóttir et al., 2006). The average background DIC concentration of the Sveðja river is 0.56 mmol/kg (Hjartarson, 1994). The concentrations of other major anions in the Múlakvísl flood water were within the range of concentrations reported by Kristmannsdóttir et al. (2006) in the river water: 49–140,

9–22, and 87–279 μmol/kg, respectively for SO_4^{2-}, F^- and Cl^-. The concentrations of these anions in the Kaldakvísl flood water collected directly from Sveðja river were close to the background concentrations. The observation that the flood water SO_4^{2-}, F^- and Cl^- concentrations were close to their background levels suggests the non-volcanic origin of these waters. Note that flood waters formed during volcanic eruptions tend to have higher SO_4^{2-}, Cl^-, and F^- concentrations than observed before and after the floods due to input of volcanic gases (Gislason et al., 2002; Sigfússon, 2009). The observed decrease in flood water SO_4^{2-} and Cl^- concentrations during the Múlakvísl flood peak, as shown in Fig. 3, suggests that there was no supply of these elements into the water during the floods, but rather a dilution of these anions by dilute glacial melt water.

Calcium, Na, and K in the water collected from the ponds representing high discharge of the Múlakvísl flood, exceeded the upper range of the background concentrations (Kristmannsdóttir et al., 2006) by factors of 3, 4, and 2, respectively. The dissolved concentrations of the major cations Si, Al, and, Fe were, however, within the normal seasonal range. Concentrations of Sr and Mn were higher than the background range during first hours of the flood. The concentrations of major cations in the water samples collected during the Kaldakvísl flood directly from Sveðja river were slightly higher than the background concentrations reported by Hjartarson (1994). The maximum measured concentrations of Mg, K, Na, Ca, Sr, and Mn exceeded the background concentrations by factors of 1.5, 1.5, 2, 3.8, 4.5, and 8, respectively. The Si, Al, and Fe concentrations in sampled waters were close to or slightly below their background concentrations.

The concentration of dissolved organic carbon (DOC) during the Múlakvísl flood was higher than typically found in Icelandic river waters, where they do not exceed 60 μmol/kg (Gislason et al., 2003; Eiriksdottir et al., 2011, 2012a, 2013a,b). In addition, formate and acetate were present in the flood waters. Note that the background concentrations of these species are not available. Nevertheless, both the elevated DOC concentration and the presence of formate and acetate suggests that active microbiological communities were present in some of the Katla subglacial reservoirs similar to that observed in the Skaftá subglacial lakes in western Vatnajökull glacier (Marteinsson et al., 2013).

The concentration of thiosulfate ($S_2O_3^{2-}$) was within the range of that measured in surface hyrothermal waters (Kaasalainen and Stefánsson, 2011). The highest concentration (16.2 μmol/kg) was measured 2.5 h before the peak of the Múlakvísl flood and it decreased gradually with time (Table 2 and Fig. 1 in Electronic Supplement). Thiosulfate is stable in alkaline fluids but decomposes at acidic conditions (Xu and Schoonen, 1995; Xu et al., 1998). This observation suggests, therefore, that the subglacial water was alkaline before the flood occurred and had likely experienced extensive water–rock interaction.

The degree of supersaturation of the flood waters with respect to secondary minerals during Múlakvísl and Kaldakvísl floods were typical for surface- and groundwaters in basaltic terrains. According to saturation state calculations, the potential phases which could precipitate from the flood waters included aluminosilicates such as clays (gibbsite, imogolite, and kaolinite) and zeolites (heulandites, stilbite, and chabazite). The supersaturation of the flood waters with respect to carbonates during the Múlakvísl flood indicates its potential to precipitate and permanently fix carbon. The low concentration of dissolved Al in flood waters, similar to that commonly observed in natural basaltic waters, is consistent with the precipitation of Al bearing clays and zeolites at high pH (Kristmannsdottir, 1979, 1982; Gislason and Eugster, 1987; Crovisier et al., 1992; Gislason et al., 1996; Stefánsson and Gislason, 2001).

6.2. Reaction path modelling

Insight of the origins of the Múlakvísl flood waters are obtained in this study through geochemical modelling. The results of reaction path modelling are summarized in Figs. 10 and 11. To be consistent with the measured flood water DIC of 9 mmol/kg, the initial fluid for this model was assumed to be in equilibrium with CO_2 gas with a pCO_2 of 0.14 bars at 4 °C. This initial fluid was calculated to have a pH of ~3.4. As this fluid reacted incrementally with basaltic glass, the pH evolved towards and passed neutrality reaching pH of ~8 after the dissolution of ~0.01 mol (equal to 1.28 g) of basaltic glass per kg of water. The water became supersaturated with respect to a number of secondary minerals including carbonates, clays, and Fe hydroxides. The mass of secondary phases precipitating according to the model calculation during basaltic glass–water interaction is presented in Fig. 11. In the reduced system the first minerals that precipitated were siderite, later goethite, Mg-clay, and smectite, whereas in the oxidized system goethite was the first secondary phase to form. As the reaction progressed towards alkaline pH, calcite, and Ca–Mg–Fe clays were predicted to precipitate. It can be seen in Fig. 10 that the modelled fluid composition, in general, approximates well those measured in the flood waters. The modelled Fe concentration for the reduced system matched the measured flood water compositions far better than those obtained from the oxidized system. This result suggests that the fluid–basalt interaction occurred primarily below the glacier cap, isolated from atmospheric oxygen and the neutralization of the flood water took place underneath the glacier and not within the river channel. The other element concentrations were independent of the redox conditions as presented in Fig. 10. The common minerals found in low temperature basaltic soils are imogolite and allophane (Wada et al., 1992), which according to the modelling did not precipitate; however, all the other secondary minerals predicted by the simulation — see Fig. 11, are in agreement with field observations (e.g. Kristmannsdottir, 1982; Gislason and Eugster, 1987; Gislason et al., 1996; Stefánsson and Gislason, 2001; Alfredsson et al., 2013). Curiously, the measured Al composition of the fluid phase exceeded the modelled flood water Al concentration (Fig. 10), suggesting that the stability of aluminium secondary minerals may be somewhat lower than in the thermodynamic database used for the calculations. Alternatively this difference could indicate sluggish precipitation kinetics for Al-phases (c.f. Zhu and Lu, 2009; Schott et al., 2012). Close agreement between modelled and measured Ca concentration indicates that there was no significant calcite dissolution within the reservoir which could increase concentration of Ca and DIC in the sampled waters. In addition, the agreement between modelled and measured Na concentrations confirms that the basalt dissolution was the primary/major source of elements in the flood waters; Na is a good indicator of reaction progress due to its slow incorporation into secondary minerals (e.g. Gislason et al., 1996). These observations also suggest that the increased DIC measured during the peak flood originated from deep CO_2 degassing. This dissolved CO_2 was then neutralised to form HCO_3^-, primarily by basalt dissolution.

According to the geochemical modelling, ~0.01 mol (1.28 g) of basaltic glass per kg of water dissolved to obtain an agreement between modelled and observed flood water compositions (Figs. 10 and 11). Taking account the Oelkers and Gislason (2001) basaltic glass dissolution rate expression (Eq. (3)), the duration of fluid—basalt interaction can be estimated if the basalt surface area is known. By multiplying the maximum measured suspended particulate concentration of 47 g/L with its BET surface area of 22.5 m^2/g, as measured in sample 2011-09-07_1220, one obtains a basalt surface area of 1057 m^2/L. By adopting this surface area, approximately 1.5 years would have been required to dissolve 0.01 mol of basaltic glass at 4 °C. These time estimates and element concentrations comparisons suggest that the chemical composition of the flood water evolved for significant time within the subglacial reservoir prior to the flood. This further implies that a volcanic eruption did not trigger the flood because the time required to neutralize the flood waters by water–rock interaction far exceeds the time this water was present in the river channel.

Note that, as is always the case, significant uncertainties are associated with geochemical modelling calculations. Uncertainties associated with the modelling calculations performed in this study include (1) the choice of initial reactive fluids, in this case the initial DIC

concentration chosen for the modelling calculation, (2) the choice of basalt surface area (note that the surface area of suspended particles can be far greater than that of other natural particles and rocks; Gislason and Eugster, 1987; Eiriksdottir et al., 2013b), (3) the choice of thermodynamic databases (c.f. Oelkers et al., 2009), (4) the choice of mineral reacting with the flood water (note that basaltic glass was the only phase assumed to dissolve, even though secondary minerals were present), (5) the choice of those secondary phases attaining local equilibrium with the fluid (c.f. Zhu and Lu, 2009), and (6) the assumption that secondary minerals attain local equilibrium (Saldi et al., 2012; Schott et al., 2012). Nevertheless the close correspondence between the geochemical model calculations and the field observations support strongly the model calculations presented in this study.

6.3. Controls on the toxicity of flood water chemistry

The heat driving glacier melting can have geothermal and/or volcanic origin. Volcanic activity has been shown to cause toxification of surface waters. For example, Flaathen and Gislason (2007) confirmed the increased toxicity of surface waters associated with the 1999 and 2000 Mt. Hekla eruption. The interaction of melted snow with salts adsorbed on the fresh ash decreased pH and increased dissolved Fe, Al, and F concentrations in surface waters so that they exceeded the allowable drinking water standards prescribed by the European Community (1998) by factors of 1350, 650, and 560, respectively. Aiuppa et al. (2000b) studied the influence of magmatic gases, especially CO_2, on groundwater chemical composition in vicinity of the Mt. Etna volcano. They showed that the inflow of magmatic CO_2 into shallow groundwaters increased basaltic host rock dissolution leading to increased trace element concentrations, which they referred to as 'natural pollution'. Some dissolved elements, notably As, Se, Mo, and Cd concentrations exceeded WHO (World Health Organisation) drinking water limits (WHO, 2008).

Waters released during both glacial floods considered in this study were alkaline and non-toxic; all measured element concentrations were below WHO drinking water standards (WHO, 2008) or the Icelandic Directorate threshold for category III surface water (IcD, 1999). This suggests that (1) the direct input of acid gases (e.g. CO_2, SO_2, HCl, HF) to the flood waters was limited and/or (2) sufficient water-basalt interaction occurred to neutralize the fluids. Enhanced dissolution and dissociation of magmatic gases would lower water pH and provoke the release of toxic metals from dissolving basalt. The higher the concentration of dissolved acid gases, the more basalt dissolution required for its neutralization. The composition of the flood waters described in this study, having high pH and DIC and low SO_4, Cl and F concentrations, were similar to Icelandic geothermal waters (e.g. Kaasalainen, 2012; Kaasalainen and Stefánsson, 2012) confirming their neutralization by long term water–rock interaction and the potential for co- precipitation of toxic metals in secondary phases such as Al, Fe hydroxides and clays.

6.4. Particulate material transport

Studies on the global cycles of the elements have been focused mainly on the river dissolved rather than particulate element fluxes. However, dissolved transport of elements to the ocean is more significant only for Na (Oelkers et al., 2012). The transport of other metals is dominated by the particulate flux; approximately 1 Gt/year of dissolved flux and 15–20 Gt/year of the suspended flux are carried by the rivers (Gaillardet et al., 1999, 2003). The ratios of the concentrations of selected elements in the flood waters transported in particulate and in dissolved form varied from 10^2 to $10^{7.5}$(Fig. 9). The most soluble elements such as Na, Ca, Sr, and K had the lowest ratios, up to 10^4, whereas the most immobile elements such as Ti, Al, and Fe had the highest ratios, more than 10^6. These high ratios indicate that the element flux during the floods was mostly transported as particulates; dissolved fluxes were significantly less important in overall transport budget. Due to the importance of suspended particle transport, the movement of insoluble elements such as Ti, Al, and Fe were far more affected by the floods than soluble elements such as Na, Ca, Sr, and K.

The ratio of the particulate to dissolved flux of selected elements during the floods were two to six orders of magnitude higher than the average global particulate/dissolved flux ratios reported by Oelkers et al. (2011). For example, the ratio of element concentrations in suspended particulate versus dissolved form for Si, Ca, Mg, Na, and K during the floods were only 2–2.5 orders of magnitude higher than their corresponding global ratios, whereas for trace elements such as Fe, Ti, Al, V, Mn, Sr, Ba, Cr the ratios were 3–6 orders of magnitude higher, revealing that floods increased more significantly the trace element suspended fluxes. This implies that the high discharge during the flood increased both macro and micro nutrients suspended flux but the latter was far more affected. Micronutrients play an important role in primary production, serving as catalysts for biochemical reactions (White, 1999; Eiriksdottir et al., 2013c). The highest measured concentration of suspended material during Múlakvísl flood was 47 g/L in sample 2011-09-07_1220, however, the suspended particle concentration could have been even higher at the flood peak. Nevertheless, even the measured values are dramatically higher than that commonly observed in Icelandic rivers, which depending on the discharge ranges up to a few of g/L, but does not usually exceed 1 g/L (Eiriksdottir et al., 2011, 2012a, 2013b). In addition, the major phase in the suspended particulate material was basaltic glass which is highly reactive (Gislason and Oelkers, 2003; Wolff-Boenisch et al., 2004, 2011). This particulate material, once deposited along the coast can serve as slow release fertilizer, promoting primary production for extended time periods (Gislason and Eiriksdottir, 2004; Eiriksdottir et al., 2013c). In addition, the divalent cations, especially Ca, transported in suspended material into the sea will dissolve and part of it will precipitate as carbonates, affecting the global carbon cycle (Gislason et al., 2006).

Results presented above confirm the sensitivity of element suspended flux to the discharge. Increased river discharge/runoff due to intensified rainfall and glacier melting as a result of climate change will affect the mass of suspended particulates deposited at the seacoast and therefore seawater chemistry. This will further affect the primary production and therefore the carbon and nitrogen global cycles.

7. Conclusions

There are several major conclusions that can be drawn from this study of the composition of the Múlakvísl and Kaldakvísl flood waters:

1. The waters from both flood events were non-toxic according to IcD and WHO guidelines (IcD, 1999; WHO, 2008). Although some limited quantity of acid gases, mainly CO_2, was apparently added to these waters subglacially, sufficient fluid–rock interaction occurred to neutralize them.
2. As indicated by reaction transport modelling, this neutralization likely occurred subglacially and took substantial time (at least one and a half year). These observations confirm the lack of direct interaction of magma with the subglacial water prior to the floods.
3. Compared to larger scale Icelandic floods associated with subglacial volcanic eruptions, there was no major flux of CO_2 or fixation during Múlakvísl and Kaldakvísl floods.
4. Although there was no major increase in overall dissolved element concentrations in Múlakvísl and Kaldakvísl rivers during the floods, a major increase in particulate flux was observed. This likely influences significantly the metal and nutrients long term budget at the seacoast.

Acknowledgements

The authors would like to thank associated editor Alessandro Aiuppa for his useful comments and in handling the manuscript, Evgenia Ilyinskaya and anonymous reviewer for their constructive comments which helped improve the manuscript. Sigurður P. Ásólfsson, Eric Sturkell and Reynir Ragnarsson are acknowledged for their help in

collecting the water samples. Rósa Ólafsdóttir and Þórdís Högnadóttir are gratefully thanked for their assistance in preparing the figures. The Icelandic Meteorological Office is thanked for permission to publish Fig. 2b. We thank all colleagues and co-workers in particular: Eydis Eiriksdottir, Niels Óskarsson, Domenik Wolff-Boenisch, Kiflom Gebrehiwot, Snorri Gudbrandsson, Nicole Keller and Hanna Kaasalainen. The work was funded by the Icelandic Science Foundation RANNÍS 121071-0061, the European Union through the European Marie Curie network Delta-Min Grant#PITN-GA-2008-215360, Landsvirkjun and the Institute of Earth Sciences, University of Iceland.

References

Aiuppa, A., Dongarrà, G., Capasso, G., Allard, P., 2000a. Trace elements in the thermal groundwaters of Vulcano Island (Sicily). J. Volcanol. Geotherm. Res. 98 (1–4), 189–207.

Aiuppa, A., Allard, P., D'Alessandro, W., Michel, A., Parello, F., Treuil, M., Valenza, M., 2000b. Mobility and fluxes of major, minor and trace metals during basalt weathering and groundwater transport at Mt. Etna volcano (Sicily). Geochim. Cosmochim. Acta 64 (11), 1827–1841.

Aiuppa, A., D'Alessandro, W., Federico, C., Palumbo, B., Valenza, M., 2003. The aquatic geochemistry of arsenic in volcanic groundwaters from southern Italy. Appl. Geochem. 18 (9), 1283–1296.

Aiuppa, A., Federico, C., Allard, P., Gurrieri, S., Valenza, M., 2005. Trace metal modeling of groundwater–gas–rock interactions in a volcanic aquifer: Mount Vesuvius, Southern Italy. Chem. Geol. 216 (3–4), 289–311.

Alfredsson, H.A., Oelkers, E.H., Hardarsson, B.S., Franzson, H., Gunnlaugsson, E., Gislason, S.R., 2013. The geology and water chemistry of the Hellisheidi, SW-Iceland carbon storage site. Int. J. Greenhouse Gas Control 12, 399–418.

Alho, P., Russell, A.J., Carrivick, J.L., Käyhkö, J., 2005. Reconstruction of the largest Holocene jökulhlaup within Jökulsá á Fjöllum, NE Iceland. Quat. Sci. Rev. 24 (22), 2319–2334.

Ambrosio, M., Doveri, M., Fagioli, M.T., Marini, L., Principe, C., Raco, B., 2010. Water–rock interaction in the magmatic–hydrothermal system of Nisyros Island (Greece). J. Volcanol. Geotherm. Res. 192, 57–68.

Arnórsson, S., 2000. Isotopic and chemical techniques in geothermal exploration, developmnent and use. Sampling methods, data handling, interpretation. International Atomic Energy Agency, Vienna.

Arnórsson, S., Gislason, S.R., 1994. CO_2 from magmatic sources in Iceland. Mineral. Mag. 58 (A), 27–28.

Arnórsson, S., Gunnlaugsson, E., Svavarsson, H., 1983. The chemistry of geothermal waters in Iceland. II. Mineral equilibria and independent variables controlling water compositions. Geochim. Cosmochim. Acta 47 (3), 547–566.

Arnórsson, S., Axelsson, G., Sæmundsson, K., 2008. Geothermal systems in Iceland. Jökull 58, 269–302.

Björnsson, H., 1998. Hydrological characteristics of the drainage system beneath a surging glacier. Nature 395 (6704), 771–774.

Björnsson, H., 2003. Subglacial lakes and jökulhlaups in Iceland. Glob. Planet. Chang. 35 (3–4), 255–271.

Björnsson, H., Kristannsdottir, H., 1984. The Grímsvötn Area, Vatnajökull, Iceland. Jökull 34, 25–50.

Björnsson, H., Pálsson, F., 2008. Icelandic glaciers. Jökull 58, 365–386.

Björnsson, H., Pálsson, F., Gudmundsson, M.T., 2000. Surface and bedrock topography of Mýrdalsjökull ice cap, Iceland: the Katla caldera, eruption sites and routes of Jökulhlaups. Jökull 49, 29–46.

Bourcier, W.L., Peiffer, D.W., Knauss, K.G., McKeegan, K.D., Smith, D.K., 1990. A kinetic model for borosilicate glass dissolution based on the dissolution affinity of a surface alteration layer. Mater. Res. Soc. Symp. Proc. 176, 209–216.

Brunauer, S., Emmett, P.H., Teller, E., 1938. Adsorption of gases in multimolecular layers. J. Am. Chem. Soc. 60, 309–319.

Brunner, G.W., 2010. HEC-RAS river analysis system. User's Manual, Version 4.1. US Army Corps of Engineers.Hydrologic Engineering Center.

Cioni, R., Guidi, M., Raco, B., Marini, L., Gambardella, B., 2003. Water chemistry of Lake Albano (Italy). J. Volcanol. Geotherm. Res. 120, 179–195.

Crovisier, J.L., Honnorez, J., Fritz, B., Petit, J.C., 1992. Dissolution of subglacial volcanic glasses from Iceland: laboratory study and modelling. Appl. Geochem. 7 (Supplement 1), 55–81.

Delmelle, P., Lambert, M., Dufrene, Y., Gerin, P., Óskarsson, N., 2007. Gas/aerosol–ash interaction in volcanic plumes: new insights from surface analyses of fine ash particles. Earth Planet. Sci. Lett. 259, 159–170.

Eggertsson, S., 1919. Ýmislegt smávegis viðvíkjandi Kötlugosinu 1918. Eimreiðin 25, 212–222.

Eiriksdottir, E.S., 2007. Chemical and mechanical weathering of basalt: measured and modelled data from North-East Iceland. Master Thesis at Faculty of Science University of Iceland.

Eiriksdottir, E.S., Gislason, S.R., Snorrason, Á., Harðardóttir, J., Þorláksdóttir, S.B., Axelsson, E., Sveinbjörnsdóttir, Á.E., 2011. Efnasamsetning, rennsli og aurburður straum-vatna á Austurlandi VIII. Gagnagrunnur Jarðvísindastofnunar of Veðurstofnunar. (Report RH-04-2011).

Eiriksdottir, E.S., Gislason, S.R., Snorrason, Á., Harðardóttir, J., Þorláksdóttir, S.B., Sveinbjörnsdóttir, Á.E., 2012a. Efnasamsetning, rennsli og aurburður straum-vatna á Austurlandi IX. Gagnagrunnur Jarðvísindastofnunar of Veðurstofnunar. (Report RH-05-2012a).

Eiriksdottir, E.S., Gislason, S.R., Snorrason, Á., Harðardóttir, J., Þorláksdóttir, S.B., Torssander, P., 2012b. Efnasamsetning, rennsli og aurburður straumvatna á Suðurlandi XV. Gagnagrunnur Jarðvísindastofnunar og Veðurstofunnar. (Report RH-06-2012).

Eiriksdottir, E.S., Gislason, S.R., Oelkers, E.H., 2013a. Does temperature or runoff control the feedback between chemical denudation and climate? Insights from NE Iceland. Geochim. Cosmochim. Acta 107, 65–81.

Eiriksdottir, E.S., Gislason, S.R., Oelkers, E.H., 2013b. The impact of climate on land derived nutrient flux. Mineral. Mag. 77 (5), 1032.

Eiriksdottir, E.S., Gislason, S.R., Harðardóttir, J., Þorláksdóttir, S.B., 2013c. Efnasamsetning, rennsli og aurburður straum-vatna á Suðurlandi XVI. Gagnagrunnur Jarðvísindastofnunar of Veðurstofnunar. Report RH-14-2013.

European Community, 1998. Council directive 98/83. Off. J. Eur. Communities 15, 90–112.

Federico, C., Aiuppa, A., Allard, P., Bellomo, S., Jean-Baptiste, P., Parello, F., Valenza, M., 2002. Magma-derived gas influx and water–rock interactions in the volcanic aquifer of Mt. Vesuvius, Italy. Geochim. Cosmochim. Acta 66 (6), 963–981.

Federico, C., Aiuppa, A., Favara, R., Gurrieri, S., Valenza, M., 2004. Geochemical monitoring of groundwaters (1998–2001) at Vesuvius volcano (Italy). J. Volcanol. Geotherm. Res. 133 (1–4), 81–104.

Flaathen, T.K., Gislason, S.R., 2007. The effect of volcanic eruptions on the chemistry of surface waters: the 1991 and 2000 eruptions of Mt. Hekla, Iceland. J. Volcanol. Geotherm. Res. 164 (4), 293–316.

Flaathen, T.K., Gislason, S.R., Oelkers, E.H., Sveinbjörnsdóttir, Á.E., 2009. Chemical evolution of the Mt. Hekla, Iceland, groundwaters: a natural analogue for CO_2 sequestration in basaltic rocks. Appl. Geochem. 24 (3), 463–474.

Floor, G.H., Calabrese, S., Román-Ross, G., D'Alessandro, W., Aiuppa, A., 2011. Selenium mobilization in soils due to volcanic derived acid rain: an example from Mt Etna volcano, Sicily. Chem. Geol. 289 (3–4), 235–244.

Freysteinsson, S., 1972. Jokulhlaup í Koldukvisl. Jökull 22, 83–88.

Frogner, P., Gislason, S.R., Óskarsson, N., 2001. Fertilizing potential of volcanic ash in ocean surface water. Geology 26 (6), 487–490.

Gaillardet, J., Dupré, B., Allégre, C., 1999. Geochemistry of large river suspended sediments: silicate weathering or recycled tracers? Geochim. Cosmochim. Acta 63, 4037–4051.

Gaillardet, J., Viers, J., Dupré, B., 2003. Trace elements in river waters. In: J.I. Drever, (Ed.). Surface and Groundwater, Weathering, and Soils, vol. 5. In: Holland, H.G., Turekian, K.K., (Exec. Eds.), Treatise on Geochemistry. Elsevier.

Galeczka, I., Wolff-Boenisch, D., Oelkers, E.H., Gislason, S.R., 2014. An experimental study of basaltic glass–H_2O–CO_2 interaction at 22 and 50 °C: implications for subsurface storage of CO_2. Geochim. Cosmochim. Acta 126, 123–145.

Geirsdóttir, Á., Hardardóttir, J., Sveinbjörnsdóttir, Á.E., 2000. Glacial extent and catastrophic meltwater events during the deglaciation of Southern Iceland. Quat. Sci. Rev. 19 (17–18), 1749–1761.

Gislason, S.R., Eiriksdottir, E.S., 2004. Water–rock interaction. In: Wanty, Richard B., Seal II, Robert R. (Eds.), Proceedings of the Eleventh International Symposium on Water–Rock Interaction, 27 June–2 July 2004, Saratoga Springs, New York, USA, pp. 1119–1121.

Gislason, S.R., Oelkers, E.H., 2003. Mechanism, rates, and consequences of basaltic glass dissolution: II. An experimental study of the dissolution rates of basaltic glass as a function of pH and temperature. Geochim. Cosmochim. Acta 67 (20), 3817–3832.

Gislason, S.R., Eugster, H.P., 1987. Meteoric water–basalt interactions. II: a field study in N.E. Iceland. Geochim. Cosmochim. Acta 51 (10), 2841–2855.

Gislason, S.R., Arnórsson, S., Armannsson, H., 1996. Chemical weathering of basalt in Southwest Iceland; effects of runoff, age of rocks and vegetative/glacial cover. Am. J. Sci. 296 (8), 837–907.

Gislason, S.R., Snorrason, Á., Kristmannsdóttir, H.K., Sveinbjörnsdóttir, Á.E., Torsander, P., Ólafsson, J., Castet, S., Dupré, B., 2002. Effects of volcanic eruptions on the CO_2 content of the atmosphere and the oceans: the 1996 eruption and flood within the Vatnajökull Glacier, Iceland. Chem. Geol. 190 (1–4), 181–205.

Gislason, S.R., Snorrason, Á., Eiriksdottir, Sigfússon, B., Elefsen, S.Ó., Harðardóttir, J., Gunnarsson, Á., Hreinsson, E.Ö., Torssander, P., Kardjilov, M.I., Óskarsson, N., 2003. Efnasamsetning, rennsli og aurburður straumvatna á Austurlandi, IV. Gagnagrunnur Raunvísindastofnunar of Orkustofnnunar. Raunvísindastofnun, Reykjavík. (RH-04-2003, 97 bls).

Gislason, S.R., Oelkers, E.H., Snorrason, Á., 2006. Role of river-suspended material in the global carbon cycle. Geology 34, 49–52.

Gislason, S.R., Oelkers, E.H., Eiriksdottir, E.S., Kardjilov, M.I., Gisladottir, G., Sigfusson, B., Snorrason, A., Elefsen, S., Hardardottir, J., Torssander, P., Óskarsson, N., 2009. Direct evidence of the feedback between climate and weathering. Earth Planet. Sci. Lett. 277, 213–222.

Gislason, S.R., Hassenkam, T., Nedel, S., Bovet, N., Eiriksdottir, E.S., Alfredsson, H.A., Hem, C.P., Balogh, Z.I., Dideriksen, K., Óskarsson, N., Sigfusson, B., Larsen, G., Stipp, S.L.S., 2011. Characterization of Eyjafjallajökull volcanic ash particles and a protocol for rapid risk assessment. PNAS 108, 7307–7312.

Gudmundsson, M.T., Högnadóttir, T., 2007. Volcanic systems and calderas in the Vatnajökull region, central Iceland: constraints on crustal structure from gravity data. J. Geodyn. 43 (1), 153–169.

Gudmundsson, M.T., Högnadóttir, T., 2011. Upptök of stærð jökulhlaups í Mulakvisl – niðurstöður flugmælinga. Minnisblað 13 Júlí 2011.

Gudmundsson, M.T., Sigmundsson, F., Bjornsson, H., 1997. Ice–volcano interaction of the 1996 Gjalp subglacial eruption, Vatnajokull, Iceland. Nature 389 (6654), 954–957.

Gudmundsson, M.T., Elíasson, J., Larsen, G., Gylfason, Á.G., Einarsson, P., Jóhannesson, T., Hákonardóttir, K.M., Torfason, H., 2005. Yfirlit um hættu vegna eldgosa og hlaupa frá vesturhluta Mýrdalsjökuls og Eyjafjallajökli. In: Guðmundsson, Magnús T., Gylfason, Ágúst Gunnar (Eds.), Hættumat vegna eldgosa og hlaupa frá vestanverðum Mýrdalsjökli og Eyjafjallajökli. Ríkislögreglustjórinn og Háskólaútgáfan, pp. 11–44.

Gudmundsson, M.T., Larsen, G., Höskuldsson, Á., Gylfason, Á.G., 2008. Volcanic hazards in Iceland. Jökull 58, 251–268.
Gudmundsson, M.T., Larsen, G., Sigmarsson, O., 2013. In: Sólnes, J., Sigmundsson, F., Bessason, B. (Eds.), Náttúruvá Á Íslándi. Eldgos og Jarðskjálftar. Viðlagatrygging Íslands/Háskólaútgáfan, p. 2013.
Gysi, A.P., Stefánsson, A., 2011. CO_2–water–basalt interaction. Numerical simulation of low temperature CO_2 sequestration into basalts. Geochim. Cosmochim. Acta 75 (17), 4728–4751.
Hannesdóttir, L.B., 2011. Minnisblað: Flód í Hagongulon 13. Júlí 2011. Report for Landsvirkjun Power Company.
Hjartarson, Á., 1994. Vatnafarskort og grunnvatnskortlagning. Master Thesis at Faculty of Science University of Iceland.
IcD, 1999. Reglugerð: um varnir gegn mengun vatns. Icelandic Directive, Reykjavik http://www.reglugerd.is/interpro/dkm/Webguard.nsf/lookByNumber/7961999?OpenDocument, 4.7.2012.
IMO, Icelandic Meteorological Office, 2013. http://en.vedur.is/.
Jakobsson, S.P., 1979. Petrology of recent basalts of the Eastern Volcanic zone, Iceland. Acta Nat. Island. 26, 1–103.
Jones, M.T., Gislason, S.R., 2008. Rapid releases of metal salts and nutrients following the deposition of volcanic ash into aqueous environments. Geochim. Cosmochim. Acta 72 (15), 3661–3680.
Jones, M.T., Pearce, C.R., Jeandel, C., Gislason, S.R., Eiriksdottir, E.S., Mavromatis, V., Oelkers, E.H., 2012a. Riverine particulate material dissolution as a significant flux of strontium to the oceans. Earth Planet. Sci. Lett. 355–356, 51–59.
Jones, M.T., Pearce, C.R., Oelkers, E.H., 2012b. An experimental study of the interaction of basaltic riverine particulate material and seawater. Geochim. Cosmochim. Acta 77, 108–120.
Jónsson, G.P., Þórarinsdóttir, T., 2011. Hlaup í Múlakvísl 8–10. Report for Icelandic Meteorological Office. (Júlí 2011).
Kaasalainen, H., 2012. Chemistry of metals and sulphur in geothermal fluids, Iceland. Doctoral thesis Faculty of Science. University of Iceland.
Kaasalainen, H., Stefánsson, A., 2011. Sulfur speciation in natural hydrothermal waters, Iceland. Geochim. Cosmochim. Acta 75, 2777–2791.
Kaasalainen, H., Stefánsson, A., 2012. The chemistry of trace elements in surface geothermal waters and steam, Iceland. Chem. Geol. 330–331, 60–85.
Kristmannsdottir, H., 1979. Alteration of basaltic rocks by hydrothermal-activity at 100–300 °C. In: Mortland, M.M., Farmer, V.C. (Eds.), Dev. Sedimentol. Elsevier, pp. 359–367.
Kristmannsdottir, H., 1982. Alteration in the IRDP dill hole compared with other drill holes n Iceland. J. Geophys. Res. 87, 6525–6531.
Kristmannsdóttir, H., Björnsson, A., Pálsson, S., Sveinbjörnsdóttir, Á.E., 1999. The impact of the 1996 subglacial volcanic eruption in Vatnajökull on the river Jökulsá á Fjöllum, North Iceland. J. Volcanol. Geotherm. Res. 92 (3–4), 359–372.
Kristmannsdóttir, H., Gislason, S.R., Snorrason, Á., Elefsen, S.Ó., Hauksdóttir, S., Sveinbjörnsdóttir, Á., Haraldsson, H., 2006. Þróun efnavöktunarkerfis til varnar mannvirkjum við umbrot í jökli. Orkustofnun, Vatnamælingar, Reykjavík (OS-2006/014, ISBN 9979-68-206-X, 54 bls).
Lacasse, C., Sigurdsson, H., Johannesson, H., Paterne, M., Carey, S., 1995. Source of ash zone 1 in North Atlantic. Bull. Volcanol. 57, 18–32.
Larsen, G., 2000. Holocene eruptions within the Katla volcanic system, south Iceland: characteristic and environmental impact. Jökull 49, 1–28.
Louvat, P., Gislason, S.R., Allégre, C.J., 2008. Chemical and mechanical erosion rates in Iceland as deduced from river dissolved and solid material. Am. J. Sci. 308 (May), 679–726.
Maizels, J., 1997. Jökulhlaup deposits in proglacial areas. Quat. Sci. Rev. 16 (7), 793–819.
Marini, L., Vetuschi Zuccolini, M., Saldi, G., 2003. The bimodal pH distribution of volcanic lake waters. J. Volcanol. Geotherm. Res. 121, 83–98.
Marteinsson, V.T., Runarsson, A., Stefansson, A., Thorsteinsson, T., Johannesson, T., Magnusson, S.H., Reynisson, E., Einarsson, B., Wade, N., Morrison, H.G., Gaidos, E., 2013. Microbial communities in the subglacial waters of the Vatnajokull ice cap, Iceland. ISME J. 7 (2), 427–437.
Milliman, J.D., Syvitski, J.P.M., 1992. Geomorphic/tectonic control of sediment discharge to the ocean: the importance of small mountainous rivers. J. Geol. 100, 525–544.
Oelkers, E.H., Gislason, S.R., 2001. The mechanism, rates and consequences of basaltic glass dissolution: I. an experimental study of the dissolution rates of basaltic glass as a function of aqueous Al, Si and oxalic acid concentration at 25 °C and pH = 3 and 11. Geochim. Cosmochim. Acta 65, 3671–3681.
Oelkers, E.H., Gislason, S.R., Eiriksdottir, E.S., Elefsen, S.O., Hardardottir, J., 2004. The significance of suspended material in the chemical transport in rivers of NE, Iceland. In: Wanty, R.B., Seal II, R.R. (Eds.), Water Rock Interactions. Taylor & Francis Group, London, pp. 865–868.
Oelkers, E.H., Benezeth, P., Pokrovski, G.S., 2009. Thermodynamic databases for water–rock interaction. Rev. Mineral. Geochem. 70, 1–46.
Oelkers, E.H., Gislason, S.R., Eiriksdottir, E.S., Jones, M., Pearce, C.R., Jeandel, C., 2011. The role of riverine particulate material on the global cycles of the elements. Appl. Geochem. 26, S365–S369.
Oelkers, E.H., Jones, M.T., Pearce, C.R., Jeandel, C., Eiriksdottir, E.S., Gislason, S.R., 2012. Riverine particulate material dissolution in seawater and its implications for the global cycles of the elements. Compt. Rendus Geosci. 344 (11–12), 646–651.
Óladóttir, B.A., Sigmarsson, O., Larsen, G., Thordarson, T., 2008. Katla volcano, Iceland: magmatic composition, dynamics and eruption frequency as recorded by Holocene tephra layers. Bull. Volcanol. 70, 475–493.
Olsson, J., Stipp, S.L.S., Dalby, K.N., Gislason, S.R., 2013. Rapid release of metal salts and nutrients from the 2011 Grímsvötn, Iceland volcanic ash. Geochim. Cosmochim. Acta 123, 134–149.
Oskarsdottir, S.M., Gislason, S.R., Snorrason, A., Halldorsdottir, S.G., Gisladottir, G., 2011. Spatial distribution of dissolved constituents in Icelandic river waters. J. Hydrol. 397 (3–4), 175–190.
Óskarsson, N., 1980. The interaction between volcanic gases and tephra: fluorine adhering to tephra of the 1970 Hekla eruption. J. Volcanol. Geotherm. Res. 8, 251–266.
Óskarsson, N., 1981. The chemistry of Icelandic lava incrustations and the latest stage of degassing. J. Volcanol. Geotherm. Res. 22, 97–121.
Pálsson, S., Vigfusson, G.H., 1996. Results of suspended load and discharge measurements 1963–1995. National Energy Authority, Reykjavik (OS-96032/VOD-05 B).
Parkhurst, D.L., Appelo, C.A.J., 1999. User's guide to PHREEQC (Version 2) — a computer program for speciation, batch-reaction, one-dimensional transport, and inverse geochemical calculations: U.S. Geological Survey Water-Resources Investigations Report 99-4259, p. 312.
Pogge von Strandmann, P.A.E., Burton, K.W., James, R.H., van Calsteren, P., Gislason, S.R., Sigfússon, B., 2008. The influence of weathering processes on riverine magnesium isotopes in a basaltic terrain. Earth Planet. Sci. Lett. 276 (1–2), 187–197.
Roberts, M.J., Russell, A.J., Tweed, F.S., Knudsen, Ó., 2000. Ice fracturing during jökulhlaups: implications for englacial flood water routing and outlet development. Earth Surf. Process. Landf. 25 (13), 1429–1446.
Russell, A.J., Roberts, M.J., Fay, H., Marren, P.M., Cassidy, N.J., Tweed, F.S., Harris, T., 2006. Icelandic jökulhlaup impacts: implications for ice-sheet hydrology, sediment transfer and geomorphology. Geomorphology 75 (1–2), 33–64.
Russell, A.J., Tweed, F.S., Roberts, M.J., Harris, T.D., Gudmundsson, M.T., Knudsen, Ó., Marren, P.M., 2010. An unusual jökulhlaup resulting from subglacial volcanism, Sólheimajökull, Iceland. Quat. Sci. Rev. 29 (11–12), 1363–1381.
Saldi, G.D., Schott, J., Pokrovsky, O.S., Gautier, Q., Oelkers, E.H., 2012. An experimental study of magnesite precipitation rates at neutral to alkaline conditions and 100–200 °C as a function of pH, aqueous solution composition and chemical affinity. Geochim. Cosmochim. Acta 83, 93–109.
Schott, J., Oelkers, E.H., Bénézeth, P., Goddéris, Y., François, L., 2012. Can accurate kinetic laws be created to describe chemical weathering? Compt. Rendus Geosci. 344, 568–585.
Seymonds, R.B., Reed, M.H., 1993. Calculation of multicomponent chemical equilibria in gas–solid–liquid systems: calculation methods, thermochemical data, and applications to studies of high-temperature volcanic gases with examples from Mount St. Helens. Am. J. Sci. 293, 758–864.
Sigfússon, B., 2009. Reactive transport of arsenic through basaltic porous media. A PhD Thesis submitted for the degree of Doctor of Philosophy at University of Aberdeen, UK.
Sigvaldason, G.E., 1963. Influence of geothermal activity on the chemistry of three glacial rivers in southern Iceland. Jökull 13, 10–17.
Sigvaldason, G.E., 1965. The Grímsvötn area. Chemical analysis of Jökulhlaup water. Jökull 15, 125–128.
Snorrason, Á., Jónsson, P., Sigurdsson, O., Pálsson, S., Árnason, S., Víkingsson, S., Kaldal, I., 2002. November 1996 Jökulhlaup on Skeidarársandur outwash plan. Iceland. In: Martin, P., Baker, V.R., Garzón, G. (Eds.), Flood and Megaflood Processes and Deposits. Recent and Ancient Examples. Special Publ. 32 of the International Association of Sedimentologists, Blackwell Science, Oxford, pp. 55–67.
Stefánsdóttir, M.B., Gíslason, S.R., 2005. The erosion and suspended matter/seawater interaction during and after the 1996 outburst flood from the Vatnajökull Glacier, Iceland. Earth Planet. Sci. Lett. 237 (3–4), 433–452.
Stefánsson, A., Gislason, S.R., 2001. Chemical weathering of basalts, Southwest Iceland: effect of rock crystallinity and secondary minerals on chemical fluxes to the ocean. Am. J. Sci. 301 (6), 513–556.
Steinthórsson, S., Óskarsson, N., 1983. Chemical monitoring of jökulhlaup water in Skeiðará and the geothermal system in Grímsvótn, Iceland. Jökull 33, 73–86.
Steinthórsson, S., Óskarsson, N., 1986. Energetics of hydrothermal systems. Extended abstracts of Fifth International symposium on water–rock interaction, Reykjavik, Iceland, August 8–17. National Energy Authority, Orkustofnun.
Sturkell, E., Einarsson, P., Roberts, M.J., Geirsson, H., Gudmundsson, M.T., Sigmundsson, F., Pinel, V., Guðmundsson, G.B., Ólafsson, H., Stefánsson, R., 2008. Seismic and geodetic insights into magma accumulation at Katla subglacial volcano, Iceland: 1999 to 2005. J. Geophys. Res. Solid Earth 113 B03212.
Taran, Y., Rouwet, D., Inguaggiato, S., Aiuppa, A., 2008. Major and trace element geochemistry of neutral and acidic thermal springs at El Chichón volcano, Mexico: implications for monitoring of the volcanic activity. J. Volcanol. Geotherm. Res. 178 (2), 224–236.
Thordarson, T., Höskuldsson, Á., 2008. Postglacial volcanism in Iceland. Jökull 58, 197–228.
Thordarson, T., Larsen, G., 2007. Volcanism in Iceland in historical time: volcano types, eruption styles and eruptive history. J. Geodyn. 43 (1), 118–152.
Tómasson, H., 1996. The jökuhlaup from Katla in 1918. Ann. Glaciol. 22, 249–254.
Vigier, N., Gislason, S.R., Burton, K.W., Millot, R., Mokadem, F., 2009. The relationship between riverine lithium isotope composition and silicate weathering rates in Iceland. Earth Planet. Sci. Lett. 287 (3–4), 434–441.
Wada, K., Arnolds, O., Kakuto, Y., Wilding, L.P., Hallmark, C.T., 1992. Clay minerals of four soils formed in eolian and tephra materials in Iceland. Geoderma 52, 351–365.
Waitt, R.B., 2002. Great Holocene floods along Jökulsá á Fjöllum, north Iceland. In: Martin, P., Baker, V.R., Garzón, G. (Eds.), Flood and Megaflood Processes and Deposits. Recent and Ancient Examples. Special Publ. 32 of the International Association of Sedimentologists, Blackwell Science, Oxford, pp. 37–51.
White, D., 1999. The physiology & biogeochemistry of prokaryotes, 2nd ed. Oxford University Press, Oxford.

WHO, 2008. Guidelines for drinking-water quality, Third edition incorporating the first and second agenda. Recommendations, volume 1. Geneva.

Wolff-Boenisch, D., Gislason, S.R., Oelkers, E.H., Putnis, C.V., 2004. The dissolution rates of natural glasses as a function of their composition at pH 4 and 10.6, and temperatures from 25 to 74 °C. Geochim. Cosmochim. Acta 68 (23), 4843–4858.

Wolff-Boenisch, D., Wenau, S., Gislason, S.R., Oelkers, E.H., 2011. Dissolution of basalts and peridotite in seawater, in the presence of ligands, and CO_2: implications for mineral sequestration of carbon dioxide. Geochim. Cosmochim. Acta 75 (19), 5510–5525.

Xu, Y., Schoonen, M.A.A., 1995. The stability of thiosulfate in the presence of pyrite in low-temperature aqueous solutions. Geochim. Cosmochim. Acta 59, 4605–4622.

Xu, Y., Schoonen, M.A.A., Nordstrom, D.K., Cunningham, K.M., Ball, J.W., 1998. Sulfur geochemistry of hydrothermal waters in Yellowstone National Park: I. the origin of thiosulfate in hot spring waters. Geochim. Cosmochim. Acta 62, 3729–3743.

Zhu, C., Lu, P., 2009. Alkali feldspar dissolution and secondary mineral precipitation in batch systems: 3. Saturation states of product minerals and reaction paths. Geochim. Cosmochim. Acta 73 (11), 3171–3200.